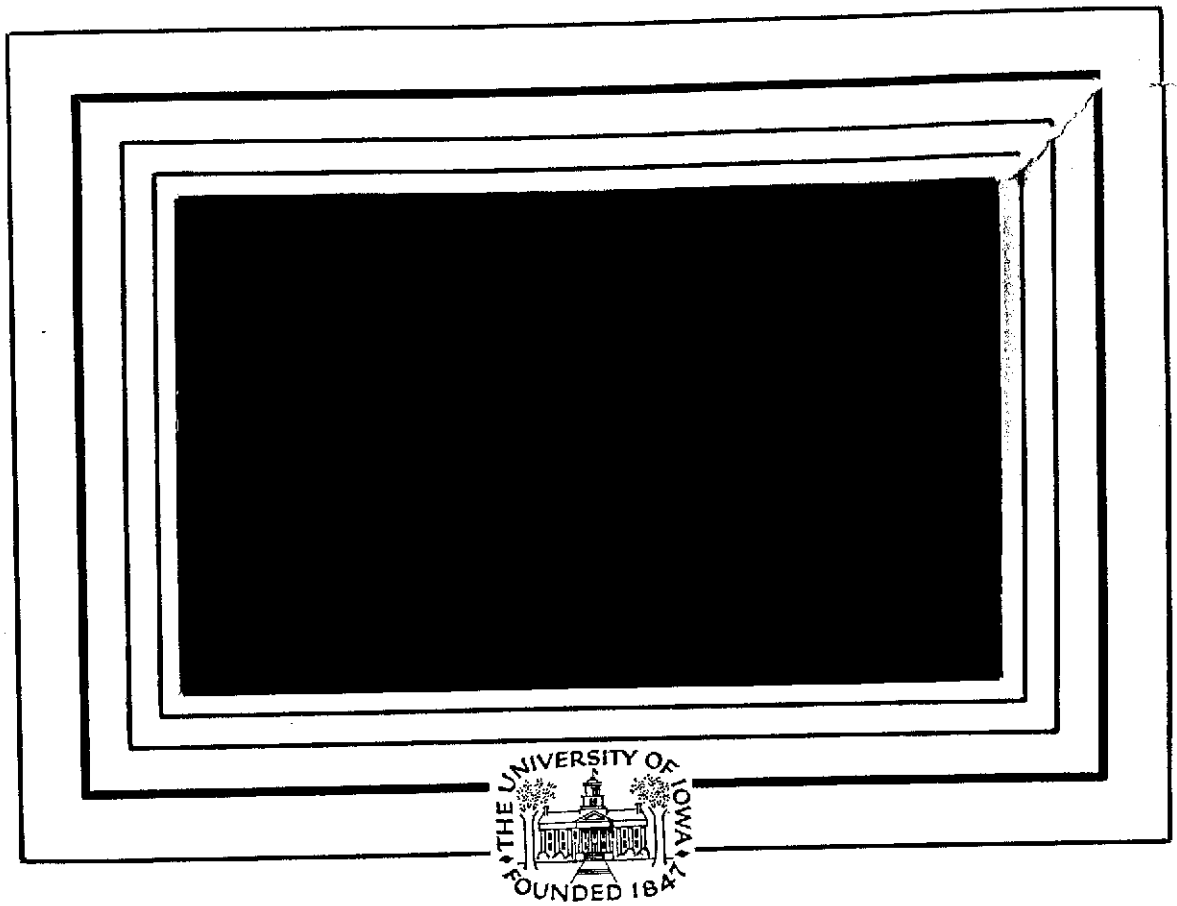

Department of Physics and Astronomy

THE UNIVERSITY OF IOWA

Iowa City, Iowa 52242

U. of Iowa 75-4

TWO-DIMENSIONAL TURBULENCE IN INVISCID FLUIDS OR GUIDING CENTER PLASMAS

C.E. Seyler, Jr.

Yehuda Salu

David Montgomery

Georg Knorr

Department of Physics and Astronomy

University of Iowa

Iowa City, Iowa 52242

January 1975

ABSTRACT

Analytic theory for two-dimensional turbulent equilibria for the inviscid Navier-Stokes equation (or the electrostatic guiding center plasma) is tested numerically. A good fit is demonstrated for the approach to a predicted energy per Fourier mode obtained from the two-temperature canonical ensemble of Kraichnan: $\langle \mid \underset{\sim}{u}(\underset{\sim}{k})\mid^2 \rangle = (\alpha + \beta k^2)^{-1}$, where $\underset{\sim}{k}$ is the wave number and α and β are reciprocal energy and enstrophy temperatures. Negative as well as positive temperature regimes are explored. Fluctuations about the mean energy per mode also compare well with theory. In the regime $\alpha < 0$, $\beta > 0$, with the minimum value of $\alpha + \beta k^2$ near zero, contour plots of the stream function reveal macroscopic vortex structures similar to those seen previously in discrete vortex simulations by Joyce and Montgomery. Kraichnan's assertion that thermodynamic limits exist for the negative temperature states is questioned. Eulerian direct interaction equations, which can be used to follow the approach to inviscid equilibrium, are derived.

I. INTRODUCTION

It is unnecessary by now to repeat justifications for studying two-dimensional models for hydrodynamic turbulence. We note, however, that among the more compelling of these is the ease with which analytical predictions can be "experimentally" tested under closely controlled circumstances by numerical solution of two-dimensional hydrodynamic equations.

Our primary purpose in this article is to describe some numerical tests we have made of the inviscid equilibrium theory of Kraichnan.[1,2,3] In Sec. II, the predictions of this theory are set down. In Sec. III, numerical results are compared with theoretical predictions. Sec. IV summarizes an analytical framework which may be used to follow the approach to equilibrium, though explorations of its consequences are deferred to a later publication. Sec. V summarizes and discusses the results.

As is by now well-known, the mathematical description applies equally well, under appropriate substitutions, to the two-dimensional electrostatic guiding center plasma and to the two-dimensional inviscid Navier-Stokes fluid. Because the theoretical predictions to be tested first arose in the hydrodynamic context, the language used here is primarily that of hydrodynamics.

II. PREDICTIONS OF THE EQUILIBRIUM INVISCID THEORY

Since there is no physical system which obeys in all particulars the two-dimensional zero-viscosity Navier-Stokes equation, it is inevitable that we shall be talking about models. The models are defined by the differential equations and the boundary conditions which govern them. Though the question of the relation of one model to another is an interesting one, arguments about which model is more "physical" can have little significant content. There are three distinct two-dimensional models which can be confused, and it is worthwhile to define each one carefully. These are: (1) the inviscid Navier-Stokes equation in position space with smooth initial data; (2) the truncated inviscid Navier-Stokes equation in Fourier-transform space with initial data which are Fourier transforms of spatially smooth functions; (3) the inviscid Navier-Stokes equation in position space with delta-function initial conditions (the Lin-Onsager discrete line-vortex model). At present, no satisfactory proofs exist that, even if various conceivable limits are taken, the results for any two of these models converge to each other for all time. Statements that one or the other is more fundamental than the others can at this point have only aesthetic significance.

First we consider the inviscid Navier-Stokes equation in two dimensions. For our purposes it is most conveniently written in dimensionless form in the vorticity representation:

$$\left(\frac{\partial}{\partial t} + \underset{\sim}{u} \cdot \nabla\right) \rho = 0 \qquad (1)$$

where $\rho = \rho(\underset{\sim}{x}, t) = \rho(x,y,t)$ is the magnitude of the vorticity vector $\underset{\sim}{\rho}(x,t) = \nabla \times \underset{\sim}{u}$, and $\underset{\sim}{u}$ is the fluid velocity. $\underset{\sim}{u}(\underset{\sim}{x},t) = \underset{\sim}{u}(x,y,t)$ has only x and y components, and nothing varies with z. $\underset{\sim}{\rho}(\underset{\sim}{x},t) = \rho\hat{b}$, where $\hat{b}$ is a unit vector in the z-direction. It is convenient to write $\underset{\sim}{u} = \hat{b} \times \underset{\sim}{E}$, where $\underset{\sim}{E} = \underset{\sim}{u} \times \hat{b} = -\nabla\phi$, and $\phi = \phi(x,y,t)$ plays the role of a stream function (electrostatic potential, in the plasma analogue). Contours of constant ϕ at fixed t are streamlines. The connection between $\underset{\sim}{E}$ and ϕ and ρ is Poisson's equation:

$$\nabla \cdot \underset{\sim}{E} = -\nabla^2\phi = \rho \quad . \qquad (2)$$

The incompressibility condition $\nabla \cdot \underset{\sim}{u} = 0$ is automatically satisfied.

Models (1) and (3) described above both obey Eqs. (1) and (2). Model (1) involves spatially smooth functions $\rho(\underset{\sim}{x},0)$, and Model (3) is distinguished from Model (1) by the presence of a discrete delta-function initial distribution of vortices, $\rho(\underset{\sim}{x},0) = \Sigma_i K_i \delta(\underset{\sim}{x}-\underset{\sim}{x}_i)$, where $\underset{\sim}{x}_i$ is the initial location of the ith vortex and K_i is its strength. Model (3) is due to Lin[4] and Onsager[5] and has been the subject of several recent publications.[6-15] At present, virtually no information exists about the general solutions of Model (1), and speculation is rife that the solutions become ill-behaved after finite times ("intermittency"), in perhaps somewhat the same way that singularities develop for the Euler equations in compressible flow. The present article is devoted to Model (2), which represents

the field variables as truncated Fourier series, in the way now to be described.

Periodic boundary conditions are assumed over a basic square box of edge L. All quantities are expanded in Fourier series,

$$\begin{aligned}
\rho(\underset{\sim}{x},t) &= \sum \rho(\underset{\sim}{k},t)\ \exp\ (i\ \underset{\sim}{k}\cdot\underset{\sim}{x}) \\
\underset{\sim}{u}(\underset{\sim}{x},t) &= \sum \underset{\sim}{u}(\underset{\sim}{k},t)\ \exp\ (i\ \underset{\sim}{k}\cdot\underset{\sim}{x}) \\
\underset{\sim}{E}(\underset{\sim}{x},t) &= \sum \underset{\sim}{E}(\underset{\sim}{k},t)\ \exp\ (i\ \underset{\sim}{k}\cdot\underset{\sim}{x}) \\
\phi(\underset{\sim}{x},t) &= \sum \phi(\underset{\sim}{k},t)\ \exp\ (i\ \underset{\sim}{k}\cdot\underset{\sim}{x}) \qquad (3)
\end{aligned}$$

where the summations extend over the set of wave vectors $\underset{\sim}{k} = (k_x, k_y) = 2\pi\ (n_x, n_y)/L$, where n_x and n_y are positive or negative integers, not both zero. Since ρ, $\underset{\sim}{u}$, $\underset{\sim}{E}$, ϕ are all real functions, reversing the sign of $\underset{\sim}{k}$ in their Fourier transforms is the same as complex conjugation. Thus the transforms are determined by giving them only over a half-space in $\underset{\sim}{k}$. The transforms are related as follows:

$$\begin{aligned}
i\ \underset{\sim}{k}\cdot\underset{\sim}{E}\ (\underset{\sim}{k},t) &= \rho(\underset{\sim}{k},t) = k^2\phi(\underset{\sim}{k},t) \\
\underset{\sim}{u}\ (\underset{\sim}{k},t) &= \hat{b}\times\underset{\sim}{E}(\underset{\sim}{k},t) \\
\text{with}\quad \underset{\sim}{k}\times\underset{\sim}{E}(\underset{\sim}{k},\ t) &= \underset{\sim}{k}\cdot\underset{\sim}{u}(\underset{\sim}{k},t) = 0\ . \qquad (4)
\end{aligned}$$

The Fourier-transformed version of Eq. (1) is conveniently written as:

$$\frac{\partial}{\partial t}\,\rho(\underset{\sim}{k},t) = \sum_{\underset{\sim}{p}+\underset{\sim}{r}=\underset{\sim}{k}} M(\underset{\sim}{r},\underset{\sim}{p})\ \rho(\underset{\sim}{r},t)\ \rho(\underset{\sim}{p},t) \qquad (5)$$

where

$$M(\underset{\sim}{r},\underset{\sim}{p}) = \frac{\hat{b} \cdot (\underset{\sim}{r} \times \underset{\sim}{p})}{2} \left\{ \frac{1}{r^2} - \frac{1}{p^2} \right\} = M(\underset{\sim}{p},\underset{\sim}{r}) \quad . \qquad (6)$$

Kraichnan's equilibrium theory[1,2] is formulated in $\underset{\sim}{k}$-space, and seems to be difficult to handle unless the number of $\underset{\sim}{k}$'s is kept finite. This question will be addressed further in Sec. III, but for present purposes, a truncation in $\underset{\sim}{k}$-space is effected by summing only over $\underset{\sim}{k}$'s which lie in a ring defined by $k_o^2 \leq |\underset{\sim}{k}|^2 = k_x^2 + k_y^2 \leq k_{max}^2$. $k_o = 2\pi/L$ and is a non-controversial lower limit provided by the box size. There appears to be no physical determination for k_{max} for a zero-viscosity fluid, but for present purposes it will be chosen as large as is compatible with available computer time. It will be remarked upon later that many of the physical predictions do not become independent of k_{max}, no matter how large k_{max} becomes. Thus what we are discussing is, strictly speaking, the statistical theory of Eq. (5), truncated in the way just described, and for the present, the precise relation to Model (1) remains unclear.

Two constants of the motion which are preserved by Eqs. (1) and (2), or (4) and (5) when periodic boundary conditions apply, are the energy density $\mathcal{E}$ and the "enstrophy" density Ω:

$$\mathcal{E} \equiv \frac{\bar{\mathcal{E}}}{V} \equiv \int E^2 \, \frac{d\underset{\sim}{x}}{V} = \sum |\underset{\sim}{E}(\underset{\sim}{k},t)|^2 = \sum |\underset{\sim}{u}(\underset{\sim}{k},t)|^2 = \sum |\rho(\underset{\sim}{k},t)|^2 k^{-2} \qquad (7)$$

$$\Omega \equiv \frac{\bar{\Omega}}{V} \equiv \int (\nabla \times \underset{\sim}{u})^2 \, \frac{d\underset{\sim}{x}}{V} = \sum k^2 \, |\underset{\sim}{E}(\underset{\sim}{k},t)|^2 = \sum k^2 \, |\underset{\sim}{u}(\underset{\sim}{k},t)|^2 = \sum |\rho(\underset{\sim}{k},t)|^2 \quad . \qquad (8)$$

The spatial volume V is given by $V = L^2$. Both $\mathcal{E}$ and Ω are constants of the motion for Eq. (5) even if the sums over $\underset{\sim}{k}$ are truncated. Many other constants of the motion implied by Eqs. (1) and (2) do not survive this truncation -- i.e., unless the sums in Eqs. (3) and (5) are allowed to range over the full infinity of permitted wave numbers, these quantities are no longer constant. It is not known whether other constants of the motion exist for the truncated version of Eq. (5) besides $\mathcal{E}$ and Ω. The indications of Sec. III, it will be seen, are that there are not.

Though Eqs.(5) with a finite set of $\underset{\sim}{k}$'s apparently do not define a Hamiltonian system, they do permit the introduction of a "phase space" whose coordinates are the real and imaginary parts of the Fourier coefficients.[16] A Liouville equation can be proved in this phase space, opening the possibility of "ensembles," or stationary probability distributions in the phase space, from which expectation values, or "ensemble averages," of physical quantities can be computed. The hope is that these expectation values will be good predictions for individual realizations of the turbulent field in the way that has become familiar in the statistical mechanics of systems of classical Hamiltonian particles.

Kraichnan proposes[1,2] a canonical ensemble as the appropriate distribution for thermal equilibrium.[17] Abbreviating the different Fourier coefficients symbolically as $\underset{\sim}{u}(\underset{\sim}{k}_1)$, $\underset{\sim}{u}(\underset{\sim}{k}_2)$, ..., the canonical ensemble is defined by the probability distribution

$$P\left(\underset{\sim}{u}\left(\underset{\sim}{k}_1\right), \underset{\sim}{u}\left(\underset{\sim}{k}_2\right), \cdots\right) = c \exp\left(-\alpha \mathcal{E} - \beta\Omega\right)$$
$$= c \exp\left\{-\sum \left(\alpha + \beta k^2\right) \left| \underset{\sim}{u}\left(\underset{\sim}{k}\right)\right|^2\right\} \qquad (9)$$

where c is a normalizing constant chosen so that

$$\int d\, \underset{\sim}{u}(k_1)\, d\, \underset{\sim}{u}\left(\underset{\sim}{k}_2\right) \cdots P = 1 \quad . \qquad (10)$$

The real and imaginary parts of $\underset{\sim}{u}\left(\underset{\sim}{k}\right) = u_r\left(\underset{\sim}{k}\right) + i\, u_i\left(\underset{\sim}{k}\right)$ are to be integrated independently, subject to the constraints that $\underset{\sim}{k} \cdot \underset{\sim}{u}\left(\underset{\sim}{k}\right) = 0$ (i.e., for each $\underset{\sim}{k}$, only one direction for the vector $\underset{\sim}{u}\left(\underset{\sim}{k}\right)$ is permitted) and that $\underset{\sim}{u}\left(\underset{\sim}{k}\right) = \underset{\sim}{u}^*\left(-\underset{\sim}{k}\right)$ (i.e., that the independent $\underset{\sim}{u}\left(\underset{\sim}{k}\right)$'s are just defined over a half space in $\underset{\sim}{k}$). α and β are constants, possibly negative, chosen to satisfy

$$\int d\, \underset{\sim}{u}\left(\underset{\sim}{k}_1\right) d\, \underset{\sim}{u}\left(\underset{\sim}{k}_2\right) \cdots \left\{\sum \left|\underset{\sim}{u}\left(\underset{\sim}{k}\right)\right|^2\right\} P = \mathcal{E} \qquad (11)$$

and

$$\int d\, \underset{\sim}{u}\left(\underset{\sim}{k}_1\right) d\, \underset{\sim}{u}\left(\underset{\sim}{k}_2\right) \cdots \left\{\sum k^2 \left|\underset{\sim}{u}\left(\underset{\sim}{k}\right)\right|^2\right\} P = \Omega \quad . \qquad (12)$$

α^{-1} and β^{-1} define two "temperatures," one for energy and one for enstrophy. Obviously, from Eq. (4), the same statistics apply to the $\left|\underset{\sim}{E}\left(\underset{\sim}{k}\right)\right|^2$ and the $\left|\rho\left(\underset{\sim}{k}\right)/k\right|^2$.

The primary purpose of Sec. III is to subject Eq. (9) to numerical test by a solution of the truncated Navier-Stokes Eq. (5) over a long enough time interval that certain average properties of the system become time independent. The most obvious quantity is the "spectrum" or spectral density

$$\left\langle \left|\underset{\sim}{u}\left(\underset{\sim}{k}\right)\right|^2 \right\rangle = \left\langle \left|\underset{\sim}{E}\left(\underset{\sim}{k}\right)\right|^2 \right\rangle = \left(\alpha + \beta k^2\right)^{-1} \quad . \qquad (13)$$

The $\langle\ \rangle$ means an expectation value computed with Eq. (9). Since in several cases, our $\underset{\sim}{k}$'s are not densely spaced enough to replace the sums over $\underset{\sim}{k}$ by integrals, we do not follow the usual convention of multiplying the expression (13) by $\pi k\, dk$ to get an "energy spectrum." The lack of isotropy at the lower values of $\underset{\sim}{k}$ also mitigates against the use of integrated spectra.

Other predictions that follow from Eq. (9) are for the fluctuation

$$\frac{\langle(|\underset{\sim}{u}(\underset{\sim}{k})|^2 - \langle|\underset{\sim}{u}(\underset{\sim}{k})|^2\rangle)^2\rangle}{\langle|\underset{\sim}{u}(\underset{\sim}{k})|^2\rangle^2} = 1 \qquad (14)$$

and the <u>mean value</u> of $\underset{\sim}{u}(\underset{\sim}{k})$:

$$\langle\underset{\sim}{u}(\underset{\sim}{k})\rangle = 0 \quad . \qquad (15)$$

Note that Eq. (15) implies that $\langle\underset{\sim}{u}(\underset{\sim}{x},t)\ \rangle = 0$ and that $\langle\rho(\underset{\sim}{x},t)\rangle = 0$.

It is to be noted that the fluctuations are not "small," and that they do not become "smaller" as more and more $\underset{\sim}{k}$'s are included. It is one of the unhappier features of the theory that, particularly for some cases ($\alpha < 0$ and β slightly greater than $-\alpha/k_o^2$, for example), the ensemble average predictions for some physical properties may look nothing like the actual values of those properties for most of the individual systems which are the realizations of the ensemble. In the example just given, for instance, the systems which are the realizations of the ensemble all have a highly non-uniform vorticity distribution on a macroscopic scale, while the macroscopic ensemble-averaged vorticity density is zero! Thus there are differences of some significance between the ensemble average and the "most

probable state" of a system which have no parallel in the statistical mechanics of ordinary gases, for example.

Finally, note that the probability distribution for $|\underset{\sim}{u}(\underset{\sim}{k})|^2/\langle|\underset{\sim}{u}(\underset{\sim}{k})|^2\rangle$ derived from Eq. (9) ia a universal Gaussian, independent of $\underset{\sim}{k}$. It can readily be computed in any computation which computes an equilibrium set of $\underset{\sim}{u}(\underset{\sim}{k})$'s, by ensemble averaging or (making the assumption of ergodicity) by time averaging.

A number of the major features of the taxonomy of the different regimes of α and β are lost if we confine attention to $\underset{\sim}{k}$-space alone. Spectra which may appear qualitatively "similar" in $\underset{\sim}{k}$-space may represent functions which look quite different in $\underset{\sim}{x}$-space. Streamlines and contour plots of the stream function are exhibited in Sec. III as evidence to the contrary of Fox and Orszag's conclusion[18] that "nothing very interesting" distinguishes the different temperature regimes.

The ranges of permissible α and β are circumscribed by the requirement[1,2] that the expression (9) be normalizable, or that the integrals in Eq. (10) all exist. Thus, $(\alpha + \beta k^2) \mid \underset{\sim}{u}(\underset{\sim}{k})|^2$ must be a monotonically increasing function of $|\underset{\sim}{u}(\underset{\sim}{k})|^2$. This is always satisfied when $\alpha > 0$ and $\beta > 0$ (Kraichnan's Case II), is never satisfied for $\alpha < 0$ and $\beta < 0$, and may or may not be satisfied when α and β are of opposite sign. The situation for which $\alpha < 0$ and $\beta k_o^2 + \alpha > 0$ (Kraichnan's Case I) appears to be believable enough, since for all allowed $\underset{\sim}{k}$, the integrals in Eq. (10) are finite. The situation for which $\beta < 0$ and $\alpha + \beta k_{max}^2 > 0$ (Kraichnan's Case III)

is more problematical, since by including enough wave numbers in the summations, the normalizability can always be violated for specific fixed values of the two temperatures. Any claim of the existence of a thermodynamic limit, in the conventional sense of the term,[19] is dubious for α and β of opposite sign. For at fixed temperatures, the integrals which define the partition function always diverge above a certain maximum spatial volume or above a certain maximum number of degrees of freedom. This is not "thermodynamic behavior" in any sense with which we are familiar.[19] But for finite, fixed volumes and finite, fixed numbers of terms in the $\underset{\sim}{k}$-summations, the predictions of Eq. (9) are well defined, and sample cases for both Case I and Case II are included in the numerical solutions displayed in Sec. III.

The boundaries between the regimes are determined[1,2] by the parameter $k_1^2 \equiv \Omega/\mathcal{E}$. The five cases for which we exhibit solutions in Sec. III have values of Ω, $\mathcal{E}$, and k_1^2 shown in Table 1. The appropriate values of α and β are determined from the numerical solution of the relations

$$\mathcal{E} = \sum_{\underset{\sim}{k}} (\alpha + \beta k^2)^{-1}$$

$$\Omega = \sum_{\underset{\sim}{k}} k^2(\alpha + \beta k^2)^{-1} \quad . \tag{16}$$

Nowhere have we made use of integral forms for $\mathcal{E}$ and Ω. Since $\Omega/\mathcal{E}$ is the crucial number, we may sum Eq. (16) over a half-space in $\underset{\sim}{k}$, or over the full space. We sum it over a half space.

Table 1

Parameters for Numerical Solutions

RUN	CASE	$\mathcal{E}$	Ω	k_1^2	α	β
A	I	0.30	3.0	10	-116	125
B	I	0.15	3.0	20	- 91.1	118
C	II	0.08	3.0	37.5	27.5	112
D	II	0.055	3.0	54.5	597	102

The details of the computed solutions are discussed in more detail in the following section. Note that for Run C, the "threshold" run, $\mathcal{E}$ and Ω are such as to put α on the slightly negative side of the boundary, if the integral expressions are used.

Run A corresponds to a situation in which over 70 percent of the energy is predicted to go to the lowest wave number k_o: a behavior called "condensation" by Kraichnan[1,2] and the most conspicuous feature of the negative temperature states seen in numerical simulations[6-15] of the Lin-Onsager Model (3). Run B still lies in the regime $\alpha < 0$, $\beta > 0$, but the fundamental k_o contains less than half the total energy, according to Eq. (9). Run C is a threshold run for which we should have close to a k^{-2} variation of $\langle |\underset{\sim}{u}(\underset{\sim}{k})|^2 \rangle$. Run D concerns the more "conventional" regime where both temperatures are large positive numbers. No runs were carried out in Regime III, which in any case might be thought unphysical because of the sensitivity of the spectral shape to k_{max}.

III. NUMERICAL RESULTS

The methods by which Eqs. (1) and (2) are solved have been described in detail elsewhere.[20,21] The essence of the method is that Eq. (5) is solved in $\underset{\sim}{x}$-space. The right hand side is obtained by fast Fourier transforming ρ, calculating $\nabla\rho$ and $\underset{\sim}{u}$ in $\underset{\sim}{k}$-space, and transforming back to $\underset{\sim}{x}$-space at each time step. The temporal advancement is carried out by a predictor-corrector method.

Diagnostics that are readily printed out at any time step are the $|\underset{\sim}{u}(\underset{\sim}{k},t)|^2 = |\underset{\sim}{E}(\underset{\sim}{k},t)|^2$ as a function of $\underset{\sim}{k}$, and contour plots of ϕ or $\rho(\underset{\sim}{x},t) = \text{const.}$ at given fixed t. Typical initial loading consisted of choosing $\underset{\sim}{u}(\underset{\sim}{k},0) \equiv 0$ except for a few values of $\underset{\sim}{k}$. As t increased, the region of non-zero $\underset{\sim}{u}(\underset{\sim}{k},t)$ typically spread out to both larger and smaller values of $|\underset{\sim}{k}|$ than those initially excited. The initial locations of the non-zero $\underset{\sim}{u}(\underset{\sim}{k},0)$ in the k_x,k_y array, were chosen to achieve the desired ratio of Ω to $\mathcal{E}$. Usually, the region of non-zero $\underset{\sim}{u}(\underset{\sim}{k},0)$ was approximately a circular annulus, though we stress that the modes are not dense enough in $\underset{\sim}{k}$-space to avoid the necessity of summing them individually. Amplitudes $|\underset{\sim}{u}(\underset{\sim}{k},0)|$ were chosen as of the same order of magnitude, when non-zero, and the associated phases were chosen randomly. Changes in phases and amplitudes with the same $\mathcal{E}$ and Ω led to no qualitative differences in behavior. The box dimension, L, was chosen to be 2π, so that (k_x, k_y) are integers. The Fourier modes computed are defined by $k_o^2 = 1 \leq k^2 \leq k_{max}^2 = 220$,

with $k_x \geq 0$ and the modes with $k_x = 0$ and $k_y \leq 0$ omitted. (The other $\underset{\sim}{u}(\underset{\sim}{k},t)$ can all be inferred from symmetry considerations.)

Typical runs evolved toward thermal equilibrium in such a way that the time-averaged spectra show systematic variations when averaged over two hundred time steps up to a given relaxation time, after which time averages over two hundred time steps show no further systematic variation. This statement was true for all runs.

Figures 1 through 4 show spectra for runs A through D, respectively. In the panels labelled "a," initial values of the $|\underset{\sim}{u}(\underset{\sim}{k},0)|^2$ are plotted versus k^2. Averages for fixed k^2's are separate points, since more than one mode may correspond to a given value of k^2. At the high end of the spectrum, the density of modes gets so high that it is necessary to average over several adjacent modes; these averages are indicated by crosses. In panels labelled "b," the spectra at an intermediate time (indicated on the graph) are shown, averaged over two hundred time steps. In panels labelled "c," the averages of the spectra over the last two hundred time steps of the run are shown, together with the theoretical prediction of Eq. (13).

In Fig. 5, an instantaneous spectrum is shown for a typical point of Run C, and in Fig. 3c, the corresponding time average over 200 time steps is displayed. The purpose of Figs. 5 and 3c is to show the extent to which additional smoothing of the spectra is introduced by time averaging. Figure 6 shows the time history of $|\underset{\sim}{u}(\underset{\sim}{k},t)|^2$ for a

typical initially unexcited mode $(k_x, k_y) = (2,2)$ for Run B. It is seen that the mode never becomes time independent, but executes unsystematic drifts which only become regular upon time averaging. Because of the large amounts of computer time consumed by each run, ensemble averaging did not appear feasible.

The principal accuracy checks we have at our disposal are conservation of $\mathcal{E}$ and Ω. Table 2 shows the percentage of non-conservation of $\mathcal{E}$ and Ω at an intermediate time chosen as halfway between the beginning and end of the run, and at the end of the run. Also shown is the time step and total time of each run.

Table 2

Tests of Conservation Laws

Run	Total Time Steps	Δt	$\Delta\mathcal{E}/\mathcal{E}$ halfway	$\Delta\mathcal{E}/\mathcal{E}$ end	$\Delta\Omega/\Omega$ halfway	$\Delta\Omega/\Omega$ end
A*	3400	.01& .005	.2%	.2%	2.6%	2.5%
B	3400	.01	.1%	.5%	1.0%	4.2%
C	3400	.01	.1%	.1%	.3%	.8%
D	3400	.01	<.1%	<.1%	<.1%	<.1%

(*Run A had Δt = .01 for the first 1000 time steps and Δt = .005 for the last 2400 time steps.)

As previously noted, the shapes of the spectra are not qualitatively different for the two different regimes of α and β. However, rather dissimilar configurations result when the Fourier transforms are inverted and contours of constant $\phi(\underset{\sim}{x},t)$ are plotted (streamlines). In Fig. 7, (a) through (d), contours are plotted for runs A through D, respectively. The three plots for each case are the initial-value contours, the contours at an intermediate time, and the final contours. The most striking effect is one first pointed out in the finite-viscosity case by Deem and Zabusky,[22] and now commonplace[5-15] in the discrete vortex simulations. Namely, the more negative α is, the greater is the degree of long-range order, and the macroscopic configuration to which the system evolves is a pair of large counter-rotating vortices which pretty well fill up the box. For the higher values of $\Omega/\mathcal{E}$, this effect is not readily observable.

Figure 8 shows the distribution of normalized values of $|\underset{\sim}{u}(\underset{\sim}{k})|^2$ for Run A and several values of $\underset{\sim}{k}$, and the theoretical Gaussian curve which should pass through them. The level of the fluctuation $\delta_k \equiv \langle(|\underset{\sim}{u}(\underset{\sim}{k})|^2 - \langle|u(\underset{\sim}{k})|^2\rangle)^2\rangle\langle|\underset{\sim}{u}(\underset{\sim}{k})|^2\rangle^{-2}$ (which should be unity according to Eq. (14)) appears on each graph.

Figure 9 shows a plot for a spectrum which evolves strictly from a $1/k^2$ initial condition ($\alpha = 0$), the "threshold distribution" in the discrete vortex theory. Its time average and instantaneous value are shown. Figure 10 shows the effect on the final state of varying the number of allowed $\underset{\sim}{k}$'s for Run A.

IV. THE "DIRECT INTERACTION" EQUATIONS

The numerical data presented in Sec. II are to be compared with theoretical predictions of the thermal equilibrium theory implied by Eq. (9). It is also obvious that interesting physics is involved in the first parts of the runs, when the thermalization is taking place. The most successful analytical descriptions of evolving turbulence in three dimensions that have been given so far are variants of Kraichnan's "direct interaction" approximation.[23-25] It is natural to attempt to apply that theory to the two-dimensional case. Even though unanswered questions remain in justifying the basic assumptions of the theory, its relatively dramatic successes in three dimensions suggest that a fundamental advance has occurred.

Here we derive, by a route which is in some respects new,[26] a pair of coupled equations for the two-time vorticity autocorrelation in Fourier space and the "infinitessimal unit response function" G of Kraichnan in the so-called Eulerian Direct Interaction Approximation (EDIA). Consequences of this pair of equations will be explored in a later publication.

A. The Infinitessimal Unit Response Function G

By $G(\underset{\sim}{k}, \underset{\sim}{k}_o, t, t')$ we mean the change of $\rho(\underset{\sim}{k},t)$ in Eq. (5) produced by introducing a unit delta-function impulsive perturbation

in $\rho(\underset{\sim}{k}_o,t)$ at a time $t = t'$. We assume that the linearized version of Eq. (5) governs G ever after, so that

$$\frac{\partial}{\partial t} G(\underset{\sim}{k},\underset{\sim}{k}_o,t,t') - 2 \sum_{\underset{\sim}{p}+\underset{\sim}{r}=\underset{\sim}{k}} M(\underset{\sim}{r},\underset{\sim}{p})\, \rho(\underset{\sim}{r},t)\, G(\underset{\sim}{p},\underset{\sim}{k}_o,t,t')$$

$$= \delta_{Kr}(\underset{\sim}{k} - \underset{\sim}{k}_o)\, \delta(t-t') \qquad (17)$$

for $t \geq t'$, and $G \equiv 0$ for $t < t'$.

Notice that G is a different function for every realization of the ensemble (i.e., for every separate set of $\rho(\underset{\sim}{k},t)$'s). Our goal is to get an approximate expression for the ensemble average of G for an ensemble consisting of non-thermal initial distributions of the $\rho(\underset{\sim}{k},t)$.

It is helpful to split G into "diagonal" ($\underset{\sim}{k} = \underset{\sim}{k}_o$) and "off-diagonal" ($\underset{\sim}{k} \neq \underset{\sim}{k}_o$) parts, so that

$$\frac{\partial}{\partial t} G(\underset{\sim}{k}_o,\underset{\sim}{k}_o,t,t') - 2 \sum_{\underset{\sim}{p}+\underset{\sim}{r}=\underset{\sim}{k}_o} M(\underset{\sim}{r},\underset{\sim}{p})\, \rho(\underset{\sim}{r},t)\, G(\underset{\sim}{p},\underset{\sim}{k}_o,t,t') = \delta(t-t') \qquad (18)$$

for $\underset{\sim}{k} = \underset{\sim}{k}_o$, while for $\underset{\sim}{k} \neq \underset{\sim}{k}_o$ we may write (17) with the diagonal contribution singled out for special attention:

$$\frac{\partial}{\partial t} G(\underset{\sim}{k},\underset{\sim}{k}_o,t,t') - 2 \sum_{\substack{\underset{\sim}{p}+\underset{\sim}{r}=\underset{\sim}{k} \\ \underset{\sim}{p}\neq\underset{\sim}{k}_o}} M(\underset{\sim}{r},\underset{\sim}{p})\, \rho(\underset{\sim}{r},t)\, G(\underset{\sim}{p},\underset{\sim}{k}_o,t,t')$$

$$= 2M(\underset{\sim}{k} - \underset{\sim}{k}_o,\ \underset{\sim}{k}_o)\, \rho(\underset{\sim}{k} - \underset{\sim}{k}_o,t)\, G(\underset{\sim}{k}_o,\underset{\sim}{k}_o,t,t'). \qquad (19)$$

We may formally solve Eq. (19) for the off-diagonal part of G in terms of the Green's function $g_{\underset{\sim}{k}_o}(\underset{\sim}{k},t,t')$ defined by

$$\frac{\partial}{\partial t} g_{\underset{\sim}{k}_o}(\underset{\sim}{k},t,t') - 2 \sum_{\substack{\underset{\sim}{p}+\underset{\sim}{r}=\underset{\sim}{k} \\ \underset{\sim}{p} \neq \underset{\sim}{k}_o}} M(\underset{\sim}{r},\underset{\sim}{p})\, \rho(\underset{\sim}{r},t)\, g_{\underset{\sim}{k}_o}(\underset{\sim}{p},t,t') = \delta(t-t') \quad (20)$$

with $g_{\underset{\sim}{k}_o} \equiv 0$ for $t < t'$. For $\underset{\sim}{k} \neq \underset{\sim}{k}_o$, we have

$$G(\underset{\sim}{k},\underset{\sim}{k}_o,t,t') = 2 \int_{t'}^{t} ds\; g_{\underset{\sim}{k}_o}(\underset{\sim}{k},t,s)\, M(\underset{\sim}{k}-\underset{\sim}{k}_o,\underset{\sim}{k}_o)\, \rho(\underset{\sim}{k}-\underset{\sim}{k}_o,s)\, G(\underset{\sim}{k}_o,\underset{\sim}{k}_o,s,t'). \quad (21)$$

Substituting Eq. (21) into Eq. (18) gives

$$\frac{\partial}{\partial t} G(\underset{\sim}{k}_o,\underset{\sim}{k}_o,t,t') - 4 \sum_{\underset{\sim}{p}+\underset{\sim}{r}=\underset{\sim}{k}_o} M(\underset{\sim}{r},\underset{\sim}{p})\, \rho(\underset{\sim}{r},t) \int_{t'}^{t} ds\, M(\underset{\sim}{p}-\underset{\sim}{k}_o,\underset{\sim}{k}_o)$$

$$\rho(\underset{\sim}{p}-\underset{\sim}{k}_o,s)\, G(\underset{\sim}{k}_o,\underset{\sim}{k}_o,s,t')\, g_{\underset{\sim}{k}_o}(\underset{\sim}{p},t,s) = \delta(t-t') \quad , \quad (22)$$

which formally involves only the Green's function g and the diagonal part $G(\underset{\sim}{k}_o,\underset{\sim}{k}_o,s,t')$.

We wish to argue now, however, that to a good approximation $g_{\underset{\sim}{k}_o}(\underset{\sim}{k},t,t')$ and $G(\underset{\sim}{k},\underset{\sim}{k},t,t')$ are the same function, a result which is by no means obvious at this point. Notice that Eq. (20) for $g_{\underset{\sim}{k}_o}(\underset{\sim}{k},t,t')$ becomes formally <u>identical</u> with Eq. (18) for $G(\underset{\sim}{k},\underset{\sim}{k},t,t')$ if the single term with $\underset{\sim}{p} = \underset{\sim}{k}_o$ is <u>not</u> omitted from the large number of terms in the sum on the left hand side of Eq. (20). Notice also that $G(\underset{\sim}{k},\underset{\sim}{k},t,t')$ and $g_{\underset{\sim}{k}_o}(\underset{\sim}{k},t,t')$ obey identical initial conditions.

Notice finally that with the term $\underset{\sim}{p} = \underset{\sim}{k}_o$ included, the Eq. (20) defining $g_{\underset{\sim}{k}_o}(\underset{\sim}{k},t,t')$ becomes <u>independent</u> of $\underset{\sim}{k}_o$. With this single (apparently very mild) approximation, we may drop the subscript altogether and write

$$g_{\underset{\sim}{k}_o}(\underset{\sim}{k},t,t') = g(\underset{\sim}{k},t,t') = G(\underset{\sim}{k},\underset{\sim}{k},t,t'). \tag{23}$$

Eq. (22) is now an equation for G alone, and involves only $\rho(\underset{\sim}{k},t)$:

$$\frac{\partial}{\partial t} g(\underset{\sim}{k},t,t') - 4 \sum_{\underset{\sim}{p}+\underset{\sim}{r}=\underset{\sim}{k}} M(\underset{\sim}{r},\underset{\sim}{p})\, \rho(\underset{\sim}{r},t) \int_{t'}^{t} ds\, M(\underset{\sim}{p}-\underset{\sim}{k},\underset{\sim}{k}) \cdot$$

$$\rho(\underset{\sim}{p}-\underset{\sim}{k},s)\, g(\underset{\sim}{k},s,t')\, g(\underset{\sim}{p},t,s) = \delta(t-t') \tag{24}$$

We shall return to Eq. (24) after we have discussed the equation for the spectral function.

B. The Vorticity Autocorrelation Q

The second fundamental quantity for the direct interaction theory is the vorticity autocorrelation Q,

$$Q(\underset{\sim}{k},t,t') \equiv \langle \rho(-\underset{\sim}{k},t')\, \rho(\underset{\sim}{k},t) \rangle \tag{25}$$

where now the ensemble average $\langle\ \rangle$ is general, and is not an average over the equilibrium distribution (9). It is readily seen that

$$\frac{\partial}{\partial t} Q(\underset{\sim}{k},t,t') = \sum_{\underset{\sim}{p}+\underset{\sim}{r}=\underset{\sim}{k}} M(\underset{\sim}{r},\underset{\sim}{p})\, \langle \rho(-\underset{\sim}{k},t')\, \rho(\underset{\sim}{r},t)\, \rho(\underset{\sim}{p},t) \rangle \quad . \tag{26}$$

For isotropic turbulence, Q depends upon $\underset{\sim}{k}$ as a function of $|\underset{\sim}{k}|$ alone, but it is not necessary to assume isotropy yet. Clearly, what is desirable to close Eq. (26) is an approximate expression for $\langle \rho(-\underset{\sim}{k},t')\ \rho(\underset{\sim}{r},t)\ \rho(\underset{\sim}{p},t)\rangle$, where $\underset{\sim}{p}+\underset{\sim}{r}=\underset{\sim}{k}$, in terms of Q and g.

If $\rho(-\underset{\sim}{k},t')$, $\rho(\underset{\sim}{r},t)$, $\rho(\underset{\sim}{p},t)$ are distributed with independent Gaussian distributions with $\langle \rho(\underset{\sim}{k},t)\rangle = 0$, then $\langle \rho(-\underset{\sim}{k},t')\ \rho(\underset{\sim}{r},t)\ \rho(\underset{\sim}{p},t)\rangle$ will vanish identically. The evolution of Q depends upon $\rho(\underset{\sim}{k},t)$'s being distributed at least to some degree in a non-Gaussian way. We hypothesize, therefore, that $\rho(\underset{\sim}{k},t)$ consists of a "Gaussian part" $\rho_G(\underset{\sim}{k},t)$ and a "non-Gaussian part" $\delta\rho(\underset{\sim}{k},t)$ which is treated as a small perturbation: $\rho(\underset{\sim}{k},t) = \rho_G(\underset{\sim}{k},t) + \delta\rho(\underset{\sim}{k},t)$. Products of non-Gaussian parts are neglected, so that

$$\begin{aligned}\langle \rho(-\underset{\sim}{k},t')\ \rho(\underset{\sim}{r},t)\ \rho(\underset{\sim}{p},t)\rangle \cong\ & \langle \delta\rho(-\underset{\sim}{k},t')\ \rho_G(\underset{\sim}{r},t)\ \rho_G(\underset{\sim}{p},t)\rangle \\ & + \langle \rho_G(-\underset{\sim}{k},t')\ \delta\rho(\underset{\sim}{r},t)\ \rho_G(\underset{\sim}{p},t)\rangle \\ & + \langle \rho_G(-\underset{\sim}{k},t')\ \rho_G(\underset{\sim}{r},t)\ \delta\rho(\underset{\sim}{p},t)\rangle \quad . \qquad (27)\end{aligned}$$

The problem, then, is to calculate the $\delta\rho(\underset{\sim}{k},t)$ in terms of ρ_G, to carry out the averaging indicated in Eq. (27) with a Gaussian distribution assumed for ρ_G, and to substitute the result back into Eq. (26). It is ρ_G that makes the major contribution to Q.

The essence of the Kraichnan method is that the effects of the various $M(\underset{\sim}{r},\underset{\sim}{p})$ coefficients in Eq. (5) are treated as independent perturbations which induce correlations between triads of modes $\underset{\sim}{p}$, $\underset{\sim}{r}$, $\underset{\sim}{k}$. The novel feature of the perturbation theory is that the

coefficients are turned on and allowed to achieve their independent additive effects not against a background or "zeroth order" in which there is no turbulence ($\rho(\underset{\sim}{k},t) = 0$) but against a background in which all the other $\rho(\underset{\sim}{k},t)$'s are allowed to have very nearly their fully-developed values.

The last sentence can be made precise by considering a system of equations which is closely related to Eq. (5):

$$\frac{\partial}{\partial t}\,\rho(\underset{\sim}{k},t) = \sum_{\underset{\sim}{p}+\underset{\sim}{r}=\underset{\sim}{k}} \tilde{M}(\underset{\sim}{r},\underset{\sim}{p})\;\rho(\underset{\sim}{r},t)\;\rho(\underset{\sim}{p},t) \tag{28}$$

where $\tilde{M}(\underset{\sim}{r},\underset{\sim}{p})$ is the same as $M(\underset{\sim}{r},\underset{\sim}{p})$ unless $\underset{\sim}{r} = \underset{\sim}{r}_o$ and $\underset{\sim}{p} = \underset{\sim}{p}_o$, in which case $\tilde{M}(\underset{\sim}{r}_o,\underset{\sim}{p}_o) = 0$. Thus Eqs. (28) differ from Eq. (5) only by the fact that the one coefficient $M(\underset{\sim}{r}_o,\underset{\sim}{p}_o)$ has been "turned off." Assume now that the term involving $M(\underset{\sim}{r}_o,\underset{\sim}{p}_o)$ is added to the right hand side of Eq. (28) and that as a consequence ρ acquires a small increment, so that

$$\frac{\partial}{\partial t}\,[\rho(\underset{\sim}{k},t) + \delta\rho^o(\underset{\sim}{k},t)] = \sum_{\underset{\sim}{p}+\underset{\sim}{r}=\underset{\sim}{k}} M(\underset{\sim}{r},\underset{\sim}{p})\;[\rho(\underset{\sim}{r},t) + \delta\rho^o(\underset{\sim}{r},t)]$$
$$\cdot\;[\rho(\underset{\sim}{p},t) + \delta\rho^o(\underset{\sim}{p},t)] \tag{29}$$

We now subtract Eq. (28) from Eq. (29) and neglect quadratic terms in the increment $\delta\rho^o$ to get for $\underset{\sim}{k} = \underset{\sim}{k}_o$,

$$\frac{\partial}{\partial t}\,\delta\rho^o(\underset{\sim}{k}_o,t) - 2\sum_{\underset{\sim}{p}+\underset{\sim}{r}=\underset{\sim}{k}_o} M(\underset{\sim}{r},\underset{\sim}{p})\;\rho(\underset{\sim}{r},t)\;\delta\rho^o(\underset{\sim}{p},t)$$
$$= M(\underset{\sim}{r}_o,\underset{\sim}{p}_o)\;\rho(\underset{\sim}{r}_o,t)\;\rho(\underset{\sim}{p}_o,t), \tag{30}$$

and for $\underset{\sim}{k} \neq \underset{\sim}{k}_o$ we may write

$$\frac{\partial}{\partial t}\,\delta\rho^o(\underset{\sim}{k},t) - 2 \sum_{\substack{\underset{\sim}{p}+\underset{\sim}{r}=\underset{\sim}{k} \\ \underset{\sim}{r} \neq \underset{\sim}{k}_o}} M(\underset{\sim}{r},\underset{\sim}{p})\ \rho(\underset{\sim}{p},t)\ \delta\rho^o(\underset{\sim}{r},t)$$

$$= 2M(\underset{\sim}{k}-\underset{\sim}{k}_o,\underset{\sim}{k}_o)\ \rho(\underset{\sim}{k}-\underset{\sim}{k}_o,t)\ \delta\rho^o(\underset{\sim}{k}_o,t). \qquad (31)$$

We now observe a connection between Eqs. (30) and (31) and the pair (18) and (19); namely, that they are identical except in the respect that there is a source term on the right hand side of Eq. (30), but only a delta function with unit coefficient in Eq. (18). It is clear that G (or g) acts as a Green's function for the pair (30), (31), and we can write at once that

$$\delta\rho^o(\underset{\sim}{k}_o,t) = \int_o^t ds\ M(\underset{\sim}{r}_o,\underset{\sim}{p}_o)\ \rho(\underset{\sim}{r}_o,s)\ \rho(\underset{\sim}{p}_o,s)\ g(\underset{\sim}{k}_o,t,s). \qquad (32)$$

The assumption which is basic to the direct interaction theory is that the $\delta\rho$'s that are needed for Eq. (27) can be obtained by superposing independent additive expressions of the form of Eq. (32). All different values of $\underset{\sim}{r}_o$ and $\underset{\sim}{p}_o$ which satisfy $\underset{\sim}{r}_o + \underset{\sim}{p}_o = \underset{\sim}{k}_o$ are included, and the ρ's which appear on the right hand side of Eq. (32) are to be approximated by the zeroth-order Gaussian Variables ρ_G.

Replacing $\underset{\sim}{k}_o$ by $-\underset{\sim}{k}$, t by t', and dropping the superscript zero, we carry out the above program and find

$$\langle \delta\rho(-\underset{\sim}{k},t')\ \rho_G(\underset{\sim}{p},t)\ \rho_G(\underset{\sim}{r},t)\rangle = \sum_{\underset{\sim}{\ell}+\underset{\sim}{\lambda}=\underset{\sim}{k}} \int_o^{t'} ds\ M(\underset{\sim}{\ell},\underset{\sim}{\lambda})\ \langle G(-\underset{\sim}{k},t',s)$$

$$\rho_G(\underset{\sim}{p},t)\ \rho_G(\underset{\sim}{r},t)\ \rho_G(-\underset{\sim}{\ell},s)\ \rho_G(-\underset{\sim}{\lambda},s)\rangle \quad . \qquad (33)$$

The final step in obtaining the EDIA approximation to Eq. (31) consists of neglecting the correlation between G and ρ_G for the different realizations of the ensemble. That is, we replace G by $\langle G \rangle$ in Eq. (33). Using the Gaussian properties of ρ_G, we have ultimately that

$$\langle \delta\rho(-\underset{\sim}{k},t') \; \rho_G(\underset{\sim}{p},t) \; \rho_G(\underset{\sim}{r},t) \rangle = 2 \int_0^{t'} ds \; \langle g(-\underset{\sim}{k},t',s) \rangle \; M(\underset{\sim}{r},\underset{\sim}{p}) \; Q(\underset{\sim}{r},t,s) \; Q(\underset{\sim}{p},t,s) \quad . \tag{34}$$

The permutation of the arguments in Eq. (34) give three similar terms which, when added together, make Eq. (26) become

$$\frac{\partial}{\partial t} Q(\underset{\sim}{k},t,t') =$$

$$2 \sum_{\underset{\sim}{p}+\underset{\sim}{r}=\underset{\sim}{k}} M(\underset{\sim}{r},\underset{\sim}{p}) \left\{ \int_0^{t'} \langle g(-\underset{\sim}{k},t',s) \rangle \; M(\underset{\sim}{r},\underset{\sim}{p}) \; Q(\underset{\sim}{r},t,s) \; Q(\underset{\sim}{p},t,s) \; ds \right.$$

$$- \int_0^{t} \langle g(\underset{\sim}{r},t,s) \rangle \; M(\underset{\sim}{p},k) \; Q(\underset{\sim}{p},t,s) \; Q(-\underset{\sim}{k},t',s) \; ds$$

$$\left. - \int_0^{t} \langle g(\underset{\sim}{p},t,s) \rangle \; M(\underset{\sim}{k},\underset{\sim}{r}) Q(-\underset{\sim}{k},t',s) \; Q(\underset{\sim}{r},t,s) \; ds \right\} \tag{35}$$

This is one of the two EDIA equations. The other one is obtained by ensemble averaging Eq. (24). Again we ignore the correlations between ρ and G, and use ρ_G for ρ in Eq. (24). The result is, for $t \geq t'$,

$$\frac{\partial}{\partial t}\langle g(\underset{\sim}{k},t,t')\rangle + 4\sum_{\underset{\sim}{p}+\underset{\sim}{r}=\underset{\sim}{k}} M(\underset{\sim}{r},\underset{\sim}{p})\int_{t'}^{t} ds\, Q(\underset{\sim}{r},t,s)\, M(\underset{\sim}{r},\underset{\sim}{k})$$

$$\langle g(\underset{\sim}{k},s,t')\rangle\,\langle g(\underset{\sim}{p},t,s)\rangle = \delta(t-t') \qquad (36)$$

with $\langle g\rangle \equiv 0$, $t < t'$.

The equation for Q can be considerably simplified for an ensemble in equilibrium. For then $Q(\underset{\sim}{k},t,t') = Q(\underset{\sim}{k},\ t-t')$ only, and the assumption $\langle g(\underset{\sim}{k},\ t-t') = Q(\underset{\sim}{k},\ t-t')/Q(\underset{\sim}{k},0)$ reduces Eq. (35) to Eq. (36) provided that

$$\frac{M(\underset{\sim}{p},\underset{\sim}{r})}{Q(\underset{\sim}{k},0)} = \frac{M(\underset{\sim}{k},\underset{\sim}{r})}{Q(\underset{\sim}{p},0)} + \frac{M(\underset{\sim}{k},\underset{\sim}{p})}{Q(\underset{\sim}{r},0)} \qquad (37)$$

is satisfied. Equation (35) then reduces to

$$\frac{\partial Q(\underset{\sim}{k},\tau)}{\partial t} + 4\sum_{\underset{\sim}{p}+\underset{\sim}{r}=\underset{\sim}{k}} \frac{M(\underset{\sim}{p},\underset{\sim}{r})M(\underset{\sim}{k},\underset{\sim}{p})}{Q(\underset{\sim}{r},0)}\int_{0}^{\tau} ds\, Q(\underset{\sim}{k},\ \tau-s)\, Q(\underset{\sim}{p},s)\, Q(\underset{\sim}{r},s) = 0 \qquad (38)$$

where $\tau = t-t'$. We also note that Eq. (37) is satisfied uniquely by $Q(\underset{\sim}{k},0) = k^2(\alpha + \beta k^2)^{-1}$, which is the thermal equilibrium spectrum predicted by Kraichnan. Conservation of $\mathcal{E}$ and Ω are easy to prove, but an H-theorem (i.e., a proof that all solutions of the coupled equations for Q and g tend to an equilibrium) is apparently difficult to prove.

V. DISCUSSION

Numerical evidence has been offered in support of the applicability of the Kraichnan two-temperature canonical ensemble, as it relates to the truncated Fourier representation of continuous inviscid Navier-Stokes fluids in two dimensions. Spectral densities, streamlines, probability distributions for fluctuations, have been employed as diagnostics. Details of the thermalization process have been recorded on tape and are available for future comparisons with calculations of velocity autocorrelations from the direct interaction equations. The claim for the existence of a thermodynamic limit, in the sense in which the term is conventionally employed in statistical mechanics, is disputed for the situation in which either temperature is negative. Relations to the Lin-Onsager discrete-vortex model predictions remain unclear.

ACKNOWLEDGMENTS

This work was supported in part by NASA Grant NGL-16-001-043 (C.S. and D.M.) and in part by USAEC Grant AT (11-1)-2059 (Y.S. and G.K.). Most of the computing was done at the City University of New York, while D.M. was an Adjunct Professor at Hunter College. We thank Professors G. Joyce and M. Emery for some assistance with some of the computations. A valuable remark by Michelle Thompson is appreciated.

After this manuscript was typed, we received a preprint in which some of the same conclusions were reached: "Ergodic Properties of Inviscid Truncated Models of Two-Dimensional Incompressible Flows," by C. Basdevant and R. Sadourny.

FOOTNOTES

[1]R.H. Kraichnan, Phys. Fluids 10, 1417 (1967).

[2]R.H. Kraichnan, "Statistical Dynamics of Two-Dimensional Flow," submitted to J. Fluid Mech. (1974).

[3]J.R. Herring, S.A. Orszag, R.H. Kraichnan, and D.G. Fox, "Decay of Two-Dimensional Homogeneous Turbulence," submitted to J. Fluid Mech. (1974). (This paper deals exclusively with viscous flows.)

[4]C.C. Lin, On The Motion of Vortices in Two Dimensions, (University of Toronto Press, Toronto, 1943).

[5]L. Onsager, Nuovo Cimento Suppl. 6, 279 (1949).

[6]D. Montgomery, Phys. Lett. A39, 7 (1972).

[7]G. Joyce and D. Montgomery, Phys. Lett. A39, 371 (1972).

[8]J.B. Taylor, Phys. Lett. A40, 1 (1972).

[9]G. Joyce and D. Montgomery, J. Plasma Phys. 10, 107 (1973).

[10]D. Montgomery and G. Joyce, Phys. Fluids 17, 1139 (1974).

[11]C.E. Seyler, Jr., Phys. Rev. Lett. 32, 515 (1974).

[12]S.F. Edwards and J.B. Taylor, Proc. Roy. Soc. (London) A336, 257 (1974).

[13]B.E. McDonald, J. Comput. Phys. 16, 360 (1974).

[14]D.L. Book, S. Fisher, and B.E. McDonald, Phys. Rev. Lett. 34, 4 (1975).

[15]D. Montgomery, in Proceedings of the 1972 Les Houches Summer School of Theoretical Physics, to be published by Gordon and Breach, 1974.

[16]T.D. Lee, Quart. Appl. Math 10, 69 (1952).

[17]Basically what is being assumed is an ergodic behavior for the microcannonical ensemble appropriate to two independent isolating constants of the motion. A rigorous derivation of the resulting two-temperature canonical ensemble (Eq. (9)) appears not to have been carried out, but appears not to present any particular difficulties.

[18]D.G. Fox and S.A. Orszag, Phys. Fluids 16, 169 (1973).

[19]e.g., D. Ruelle, Statistical Mechanics: Rigorous Results (W.A. Benjamin, New York, 1969).

The common usage is that at fixed temperature, the thermodynamic limit is said to exist if the Helmholtz free energy per particle remains finite as the number of independent phase space coordinates and spatial volume go to infinity proportionally to each other. Manifestly, this condition is not satisfied for the present system.

[20]S.A. Orszag, Studies in Appl. Math. 50, 293 (1971).

[21]Y. Salu and G. Knorr, "Use of the Spectral Method for Two- and Three-Dimensional Guiding Center Plasmas," to be published in J. Comp. Phys.

[22]G.S. Deem and N.J. Zabusky, Phys. Rev. Letters 27, 396 (1971).

[23]R.H. Kraichnan, Phys. Rev. 113, 1181 (1959).

[24]R.H. Kraichnan, J. Fluid Mech. 5, 497 (1959).

[25]J.R. Herring and R.H. Kraichnan, in Statistical Models and Turbulence, ed. by M. Rosenblatt and C. Van Atta, (Springer-Verlag, New York, 1972), pp. 148-194.

[26]Our treatment will be seen to owe a debt to the formulation of R. Betchov, in Dynamics of Fluids and Plasmas, ed. by S. -I. Pai (Academic Press, New York, 1966), pp. 215-237.

[27]I. Cook has derived an equation similar to, but different in several important respects from Eq. (35) in J. Plasma Phys. 12, 501 (1974).

FIGURE CAPTIONS

Fig. 1 Energy spectra for Run A: (a) initially; (b) a time average over 200 time steps in the middle of the run; and (c) a time average over the last 200 time steps of the run. The solid curve is the theoretical prediction, Eq. (13). Crosses indicate averages over several closely-spaced values of k^2.

Fig. 2 Energy spectra for Run B: (a) initially; (b) a time average over 200 time steps in the middle of the run; and (c) a time average over the last two hundred time steps of the run. The solid curve is the theoretical prediction, Eq. (13). Crosses indicate averages over several closely-spaced values of k^2.

Fig. 3 Energy spectra for Run C: (a) initially; (b) a time average over 200 time steps in the middle of the run; and (c) a time average over the last two hundred time steps of the run. The solid curve is the theoretical prediction, Eq. (13). Crosses indicate averages over several closely-spaced values of k^2.

Fig. 4 Energy spectra for Run D: (a) initially; (b) a time average over 200 time steps in the middle of the run; and (c) a time average over the last two hundred time steps of the run. The solid curve is the theoretical prediction, Eq. (13). Crosses indicate averages over several closely-spaced values of k^2.

Fig. 5 Instantaneous energy spectrum for a typical point of Run C. The intention is to indicate the typical level of fluctuations about the time averaged values.

Fig. 6 Time history of $|\underset{\sim}{u}(\underset{\sim}{k},t)|$ for a typical mode: $(k_x, k_y) = (2,2)$ for Run B. The amplitude appears to pass through zero at irregular intervals.

Fig. 7 (a-d) Contours of constant ϕ (streamlines) for runs A through D. The left panels are the initial values, the center panels are the contours halfway through the runs, and the right panels are the final contours. Note the formation of large vortex structures in Run A, the case in which α is most negative.

Fig. 8 Plots of $|\underset{\sim}{u}(\underset{\sim}{k})|^2$, normalized to their time averages, for typical values of (k_x, k_y) in Run A. The solid curve is the theoretical Gaussian which should describe them according to Eq. (13).

Fig. 9 Test of the constancy of the "threshold" spectrum $|\underset{\sim}{u}(\underset{\sim}{k})|^2 \sim k^{-2}$: instaneous value and time average.

Fig. 10 The effect of using the initial conditions of Run A in the presence of two different values of the allowed number of Fourier modes. Note that the final state does not, and should not, become independent of the number of $\underset{\sim}{k}$-modes employed.

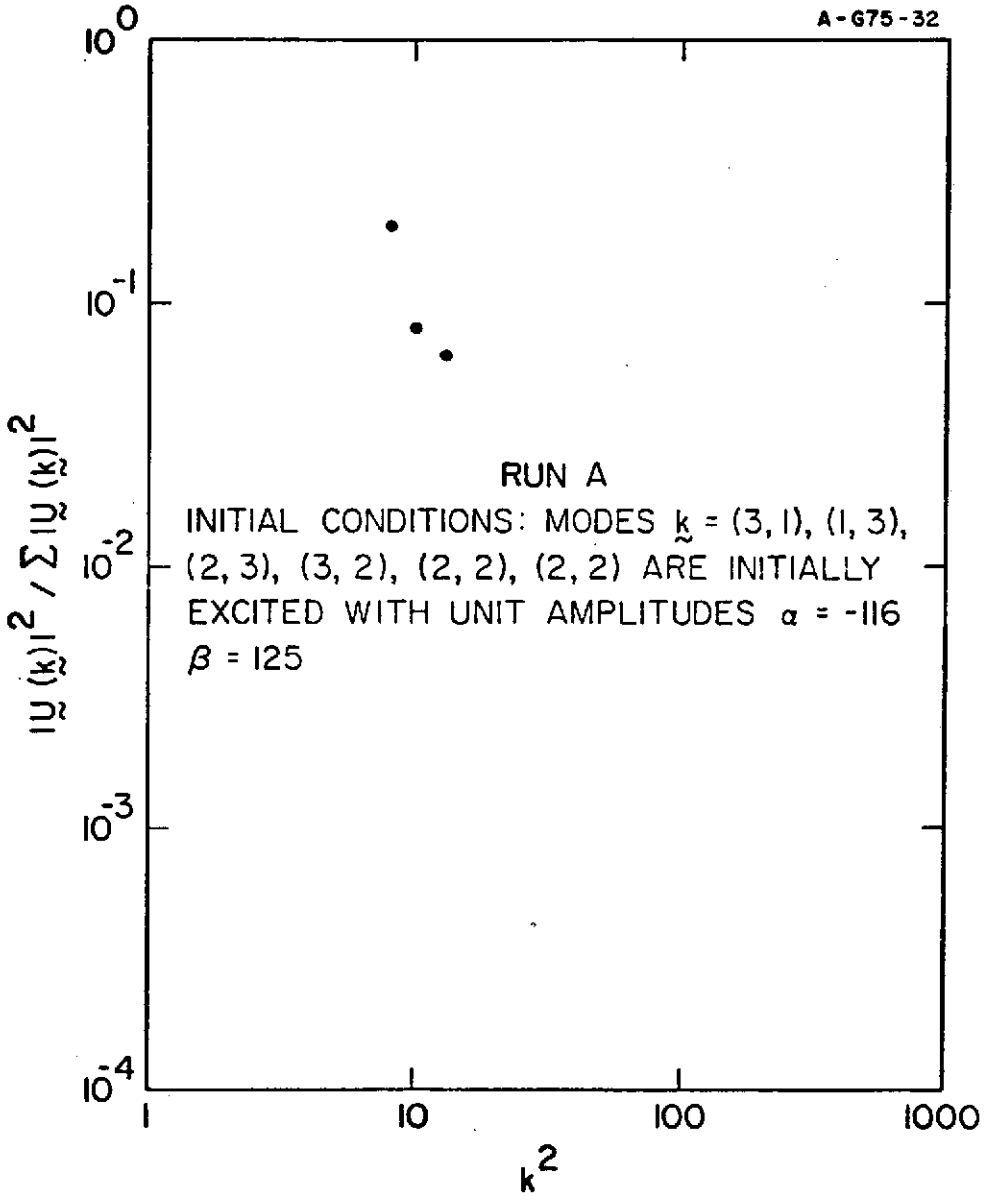
A-G75-32
10^0
10^{-1}
10^{-2}
10^{-3}
10^{-4}
$|\underset{\sim}{U}(\underset{\sim}{k})|^2 / \Sigma|\underset{\sim}{U}(\underset{\sim}{k})|^2$
RUN A
INITIAL CONDITIONS: MODES $\underset{\sim}{k}$ = (3, 1), (1, 3), (2, 3), (3, 2), (2, 2), (2, 2) ARE INITIALLY EXCITED WITH UNIT AMPLITUDES α = -116 β = 125
1
10
100
1000
k^2

Figure 1a

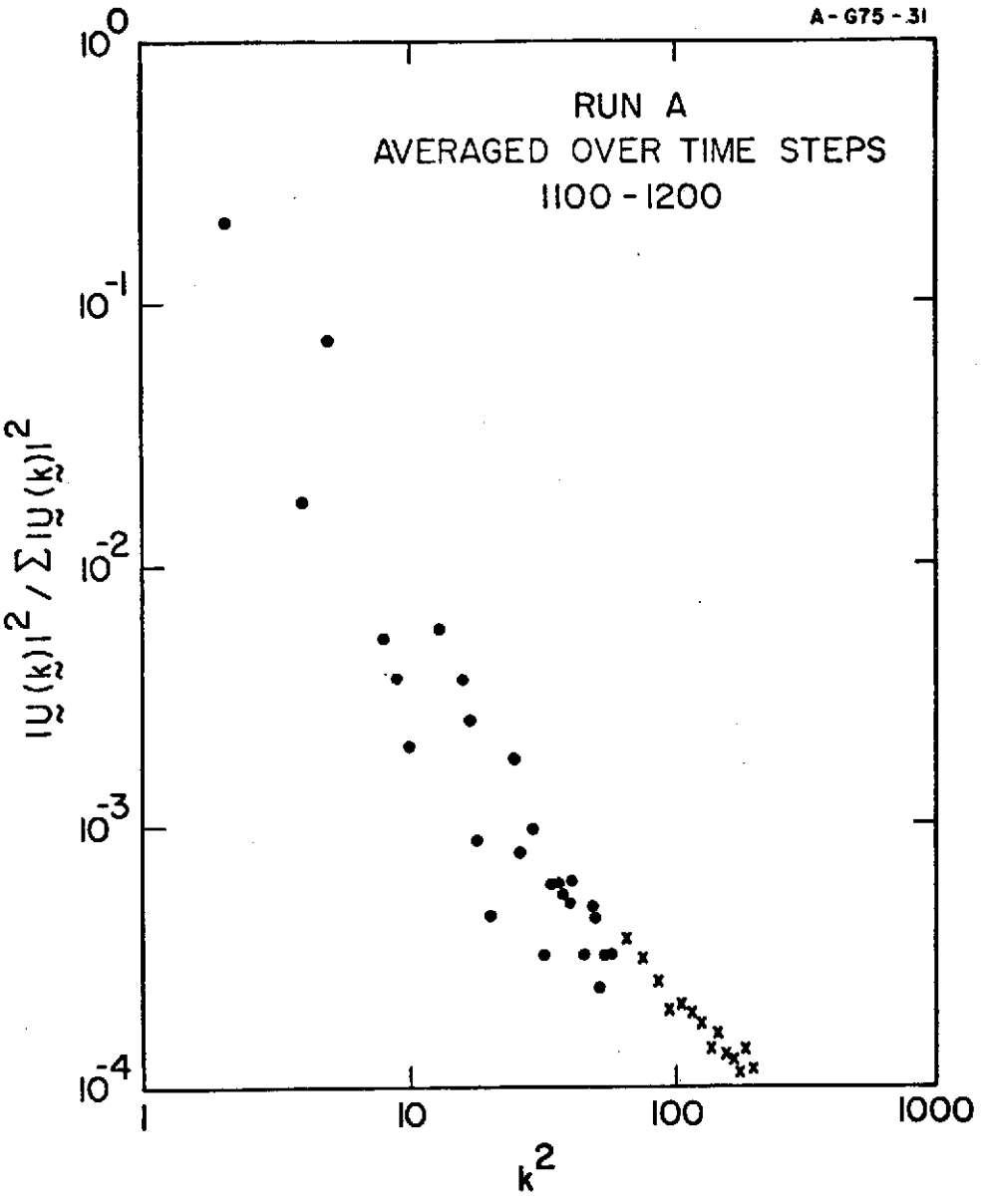
A-G75-31
RUN A
AVERAGED OVER TIME STEPS
1100 - 1200
10^0
10^{-1}
10^{-2}
10^{-3}
10^{-4}
$|\underset{\sim}{U}(\underset{\sim}{k})|^2 / \Sigma|\underset{\sim}{U}(\underset{\sim}{k})|^2$
1
10
100
1000
k^2

Figure 1b

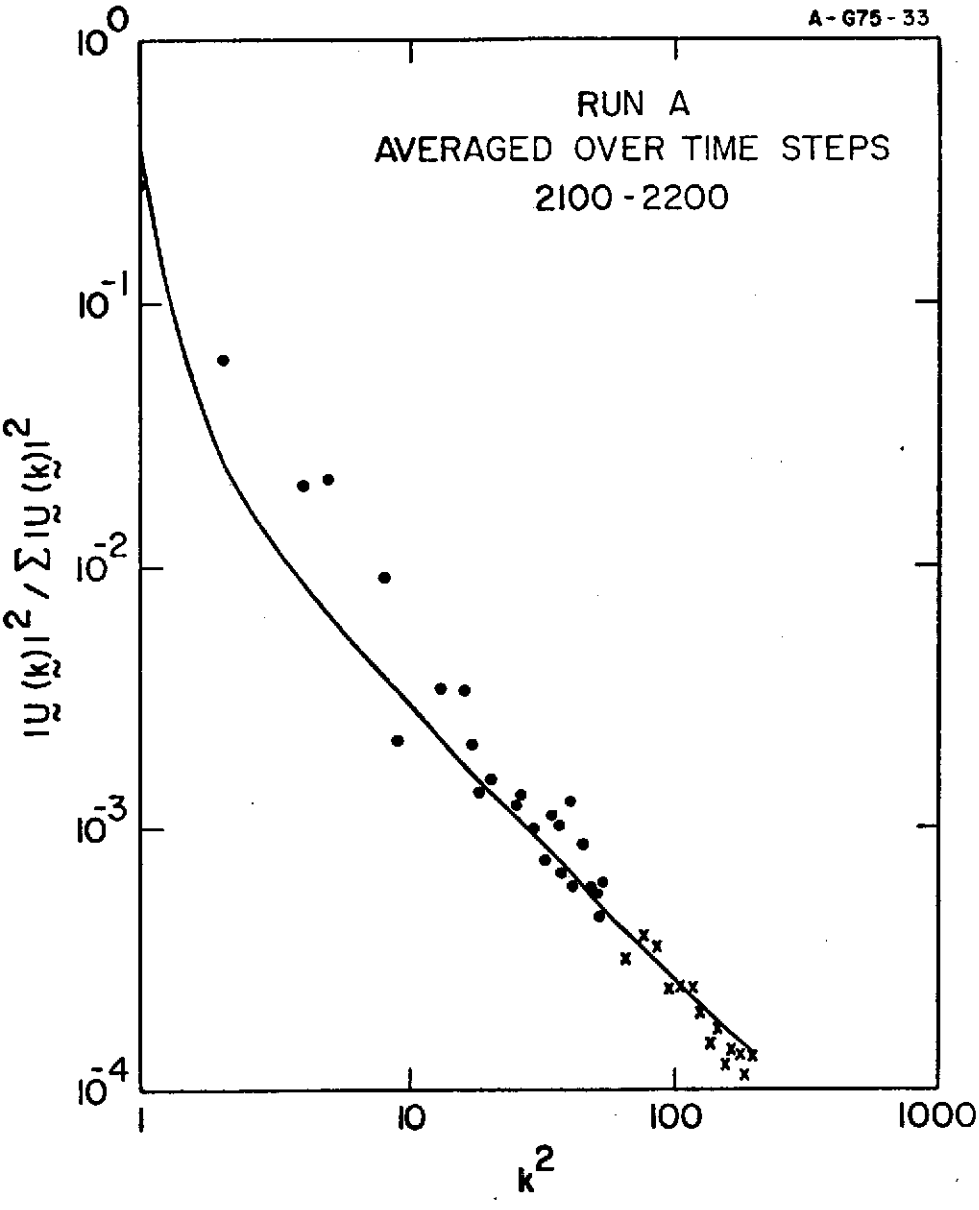
A-G75-33
RUN A
AVERAGED OVER TIME STEPS
2100 - 2200
10^0
10^{-1}
10^{-2}
10^{-3}
10^{-4}
$|\tilde{U}(k)|^2 / \Sigma |\tilde{U}(k)|^2$
1
10
100
1000
k^2

Figure 1c

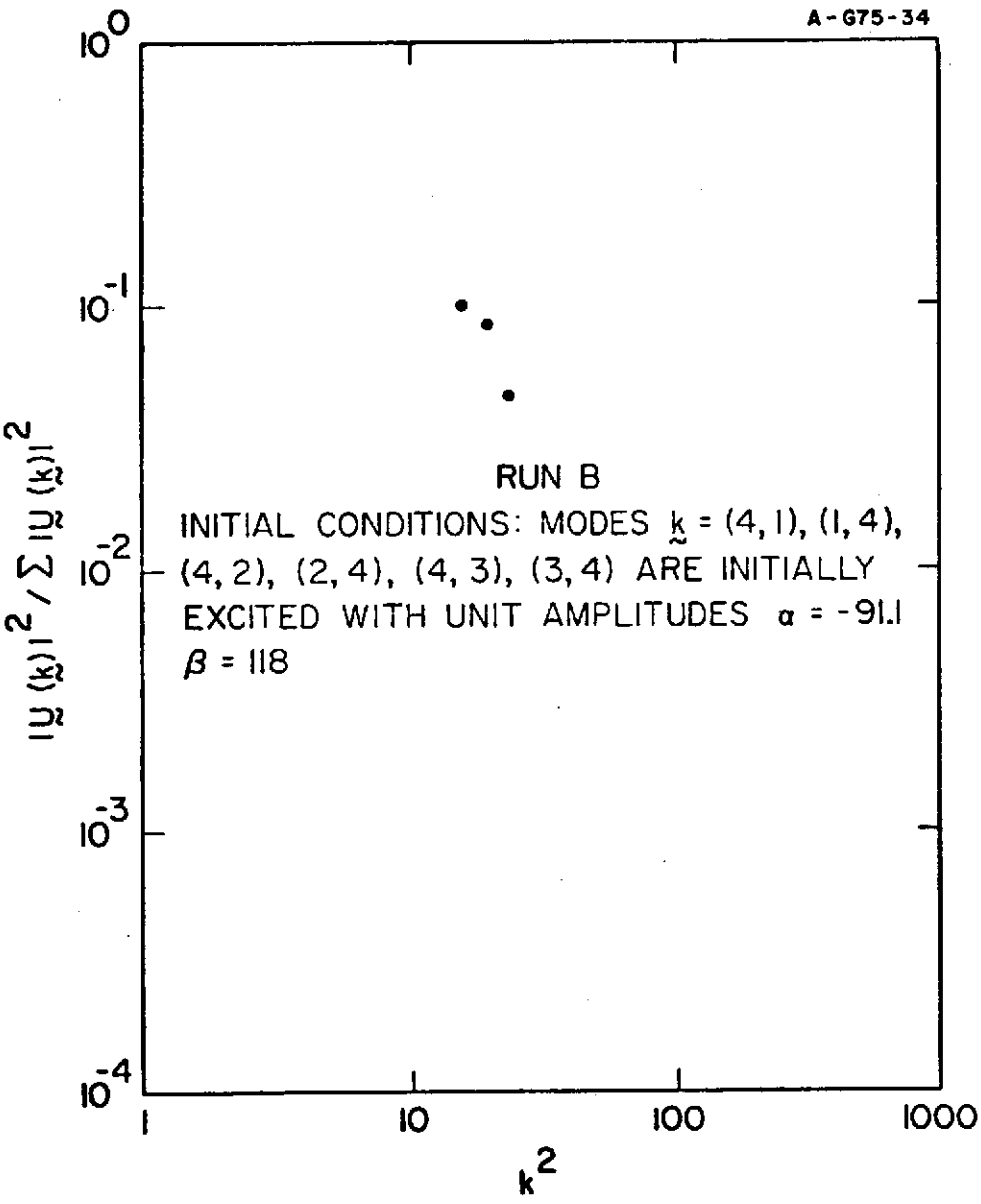
A-G75-34
10^0
10^{-1}
10^{-2}
10^{-3}
10^{-4}
$|\tilde{U}(\underset{\sim}{k})|^2 / \Sigma |\tilde{U}(\underset{\sim}{k})|^2$
RUN B
INITIAL CONDITIONS: MODES $\underset{\sim}{k}$ = (4, 1), (1, 4), (4, 2), (2, 4), (4, 3), (3, 4) ARE INITIALLY EXCITED WITH UNIT AMPLITUDES α = -91.1 β = 118
1
10
100
1000
k^2

Figure 2a

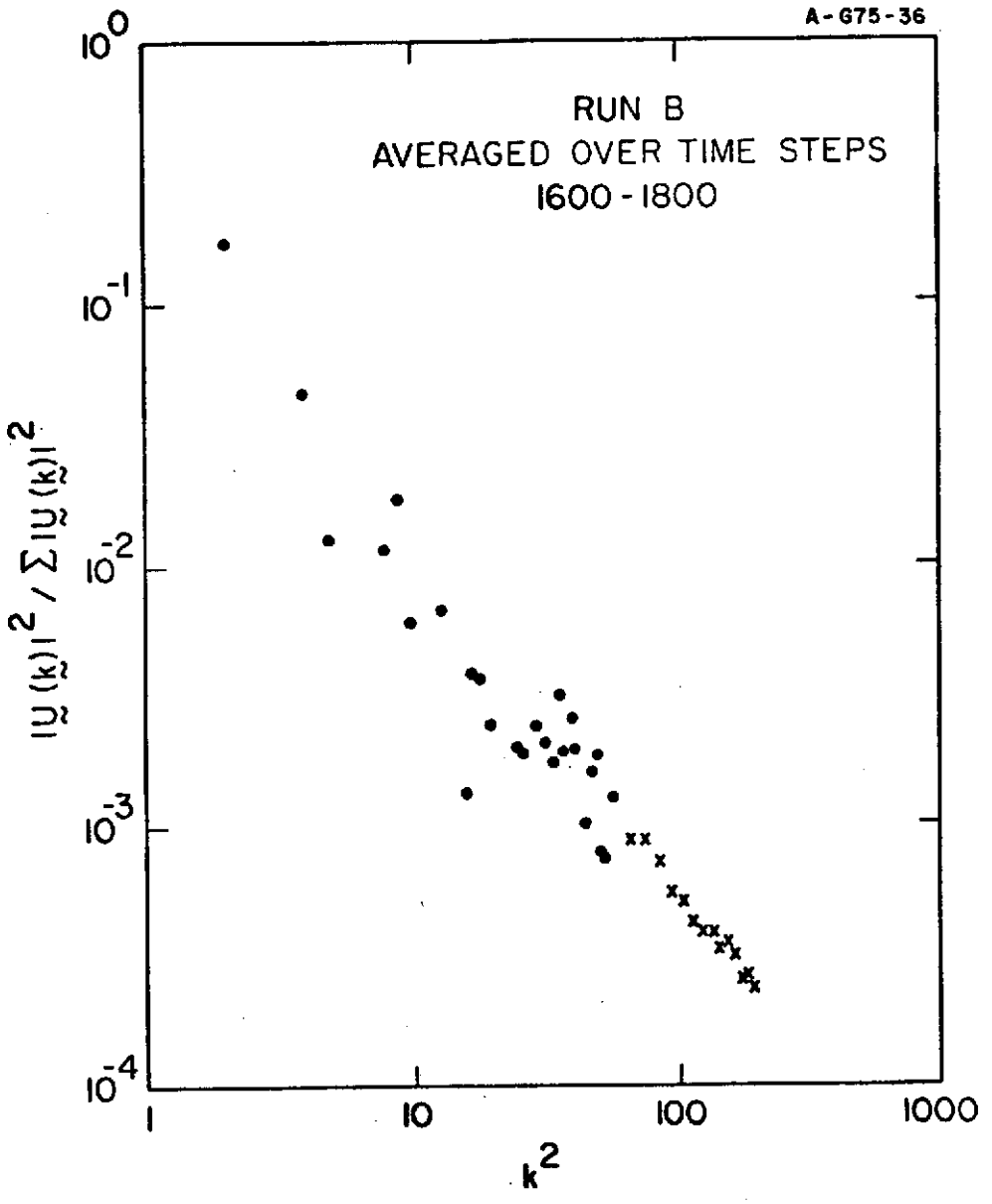
A-G75-36
RUN B
AVERAGED OVER TIME STEPS
1600 - 1800
10^0
10^{-1}
10^{-2}
10^{-3}
10^{-4}
$|\tilde{U}(k)|^2 / \Sigma|\tilde{U}(k)|^2$
1
10
100
1000
k^2

Figure 2b

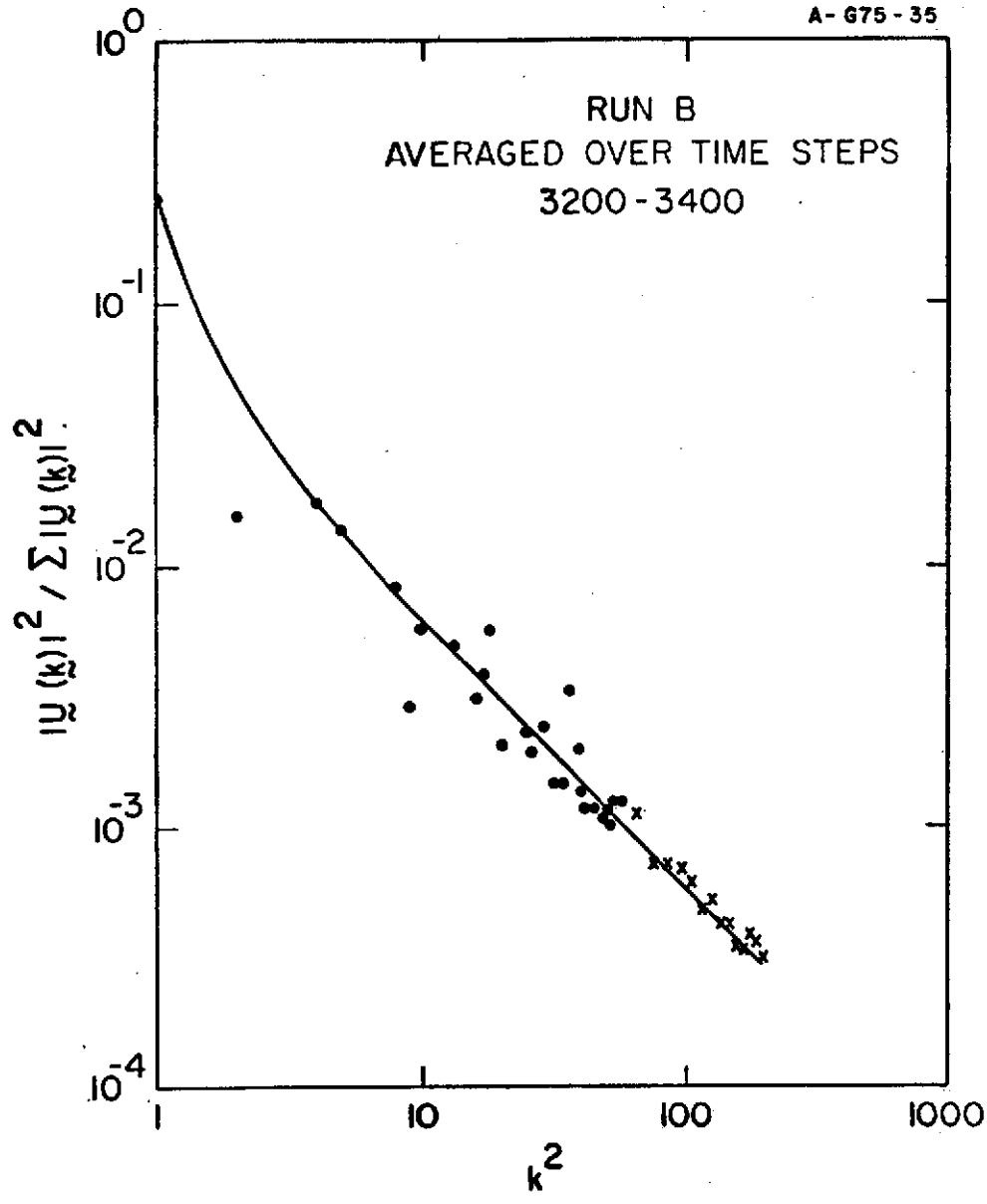
A-G75-35
RUN B
AVERAGED OVER TIME STEPS
3200-3400
10^0
10^{-1}
10^{-2}
10^{-3}
10^{-4}
$|\tilde{u}(k)|^2 / \Sigma|\tilde{u}(k)|^2$
1
10
100
1000
k^2

Figure 2c

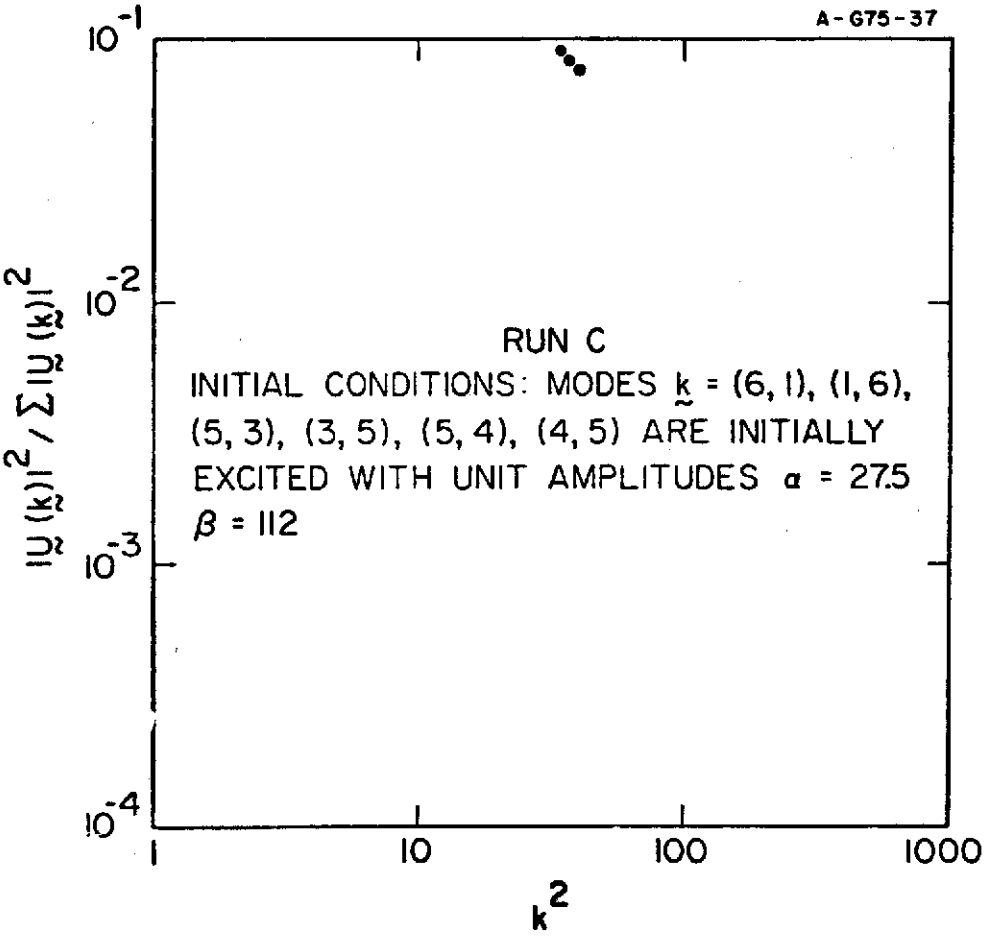
A-G75-37
10^{-1}
10^{-2}
10^{-3}
10^{-4}
$|\underset{\sim}{u}(\underset{\sim}{k})|^2 / \Sigma|\underset{\sim}{u}(\underset{\sim}{k})|^2$
RUN C
INITIAL CONDITIONS: MODES $\underset{\sim}{k}$ = (6, 1), (1, 6), (5, 3), (3, 5), (5, 4), (4, 5) ARE INITIALLY EXCITED WITH UNIT AMPLITUDES α = 27.5 β = 112
1
10
100
1000
k^2

Figure 3a

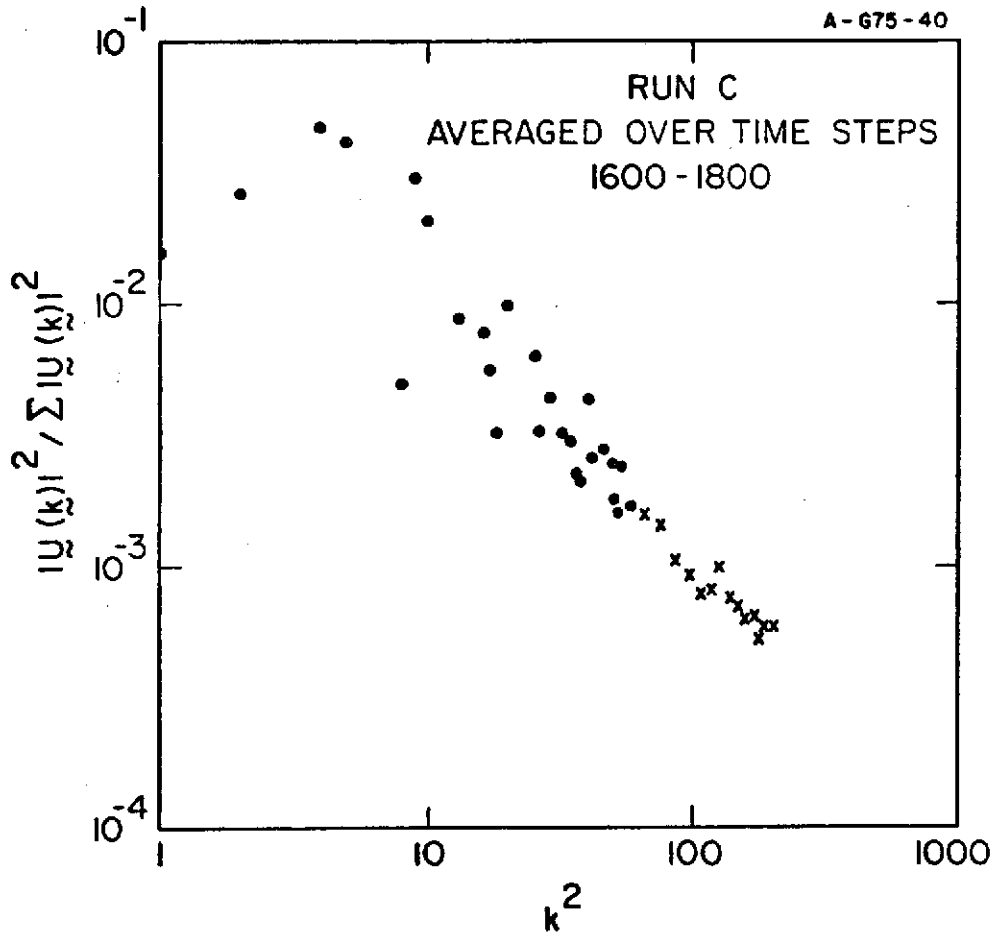
A-G75-40
RUN C
AVERAGED OVER TIME STEPS
1600 - 1800
10^{-1}
10^{-2}
10^{-3}
10^{-4}
$|\tilde{U}(k)|^2 / \Sigma |\tilde{U}(k)|^2$
1
10
100
1000
k^2

Figure 3b

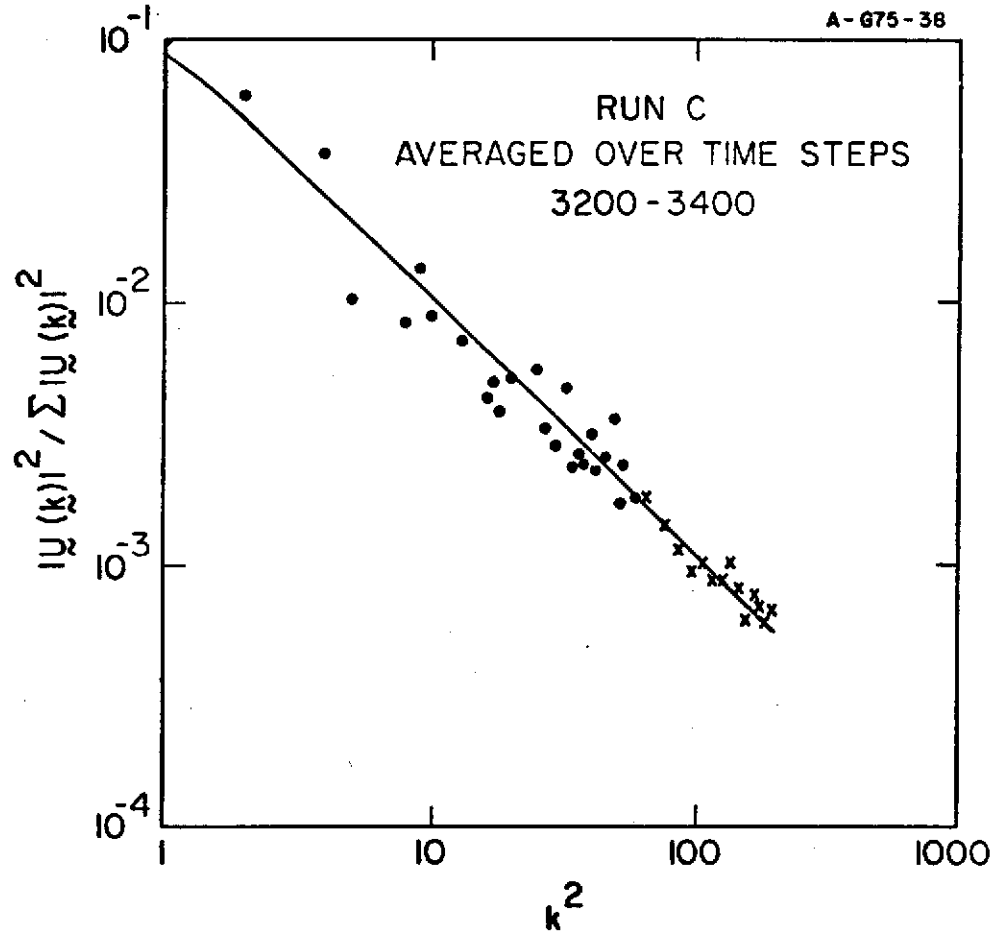
A-G75-38
RUN C
AVERAGED OVER TIME STEPS
3200-3400
10^{-1}
10^{-2}
10^{-3}
10^{-4}
$|\tilde{u}(k)|^2 / \Sigma|\tilde{u}(k)|^2$
1
10
100
1000
k^2

Figure 3c

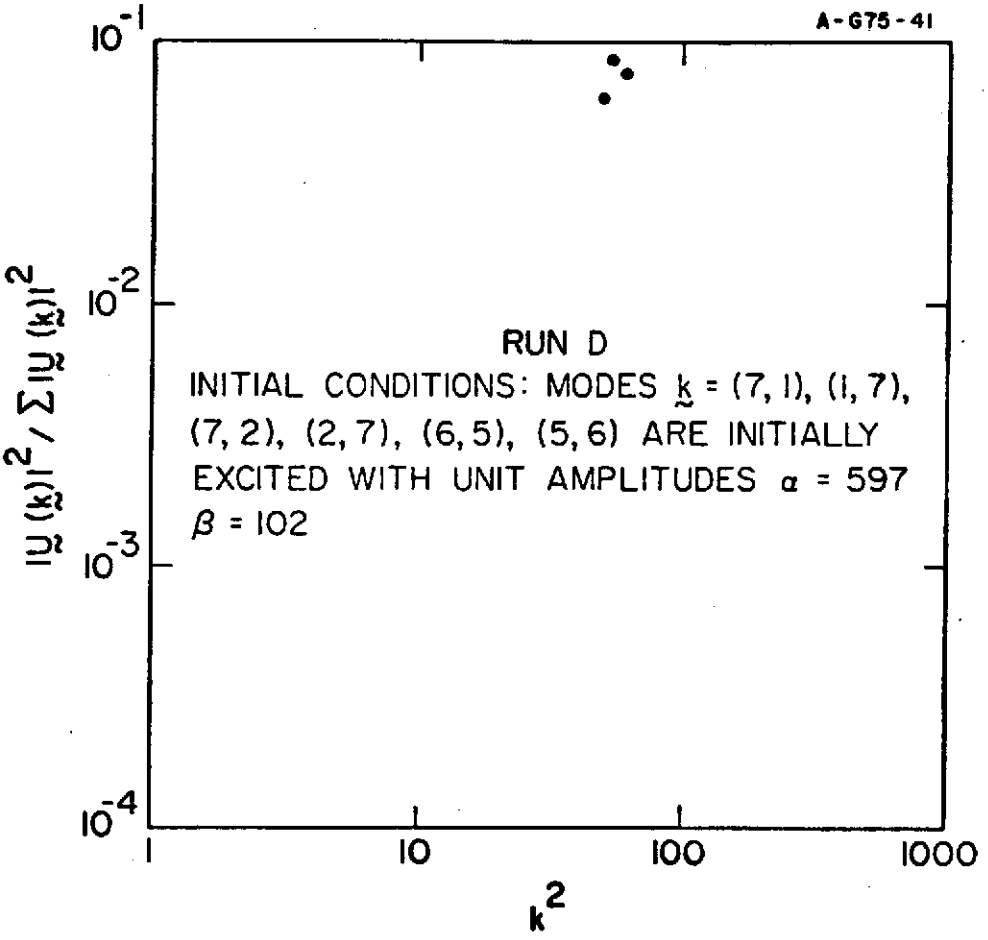
A-G75-41
10^{-1}
10^{-2}
10^{-3}
10^{-4}
$|\underset{\sim}{u}(\underset{\sim}{k})|^2 / \Sigma|\underset{\sim}{u}(\underset{\sim}{k})|^2$
RUN D
INITIAL CONDITIONS: MODES $\underset{\sim}{k}$ = (7, 1), (1, 7), (7, 2), (2, 7), (6, 5), (5, 6) ARE INITIALLY EXCITED WITH UNIT AMPLITUDES α = 597
β = 102
1
10
100
1000
k^2

Figure 4a

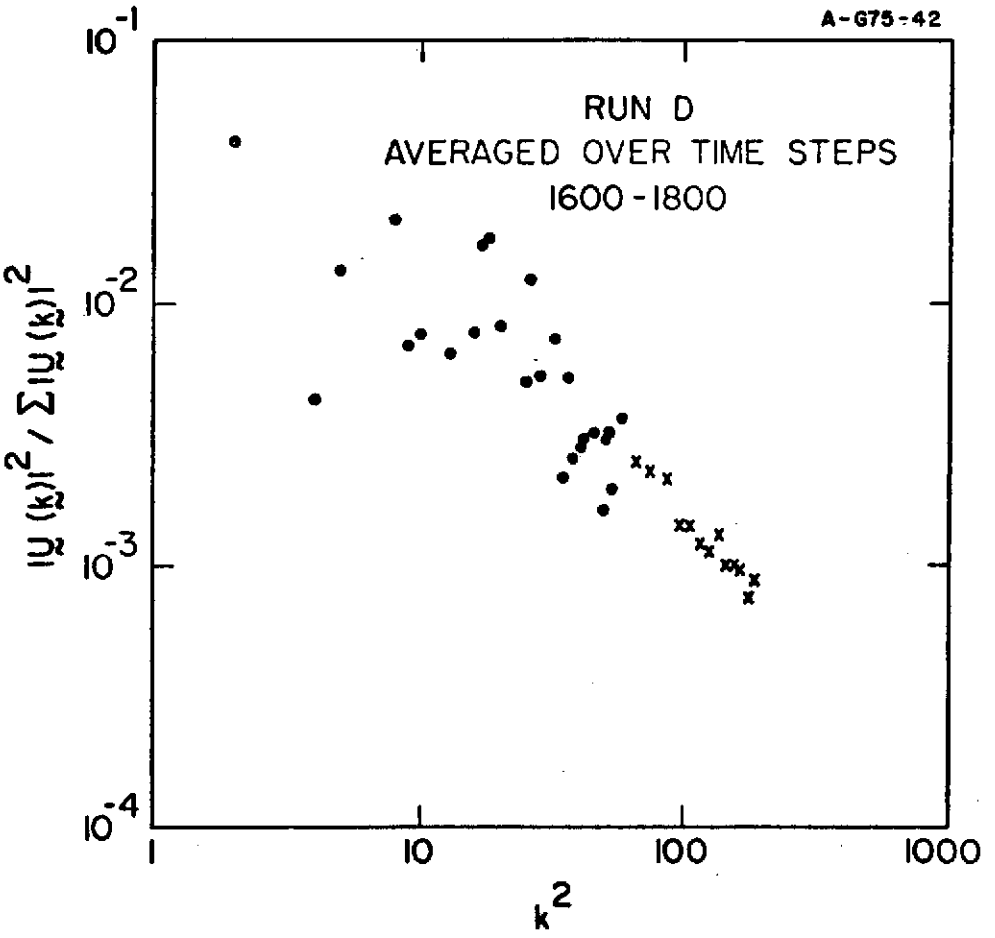
A-G75-42
RUN D
AVERAGED OVER TIME STEPS
1600 - 1800
10^{-1}
10^{-2}
10^{-3}
10^{-4}
$|\underset{\sim}{u}(k)|^2 / \Sigma|\underset{\sim}{u}(k)|^2$
1
10
100
1000
k^2

Figure 4b

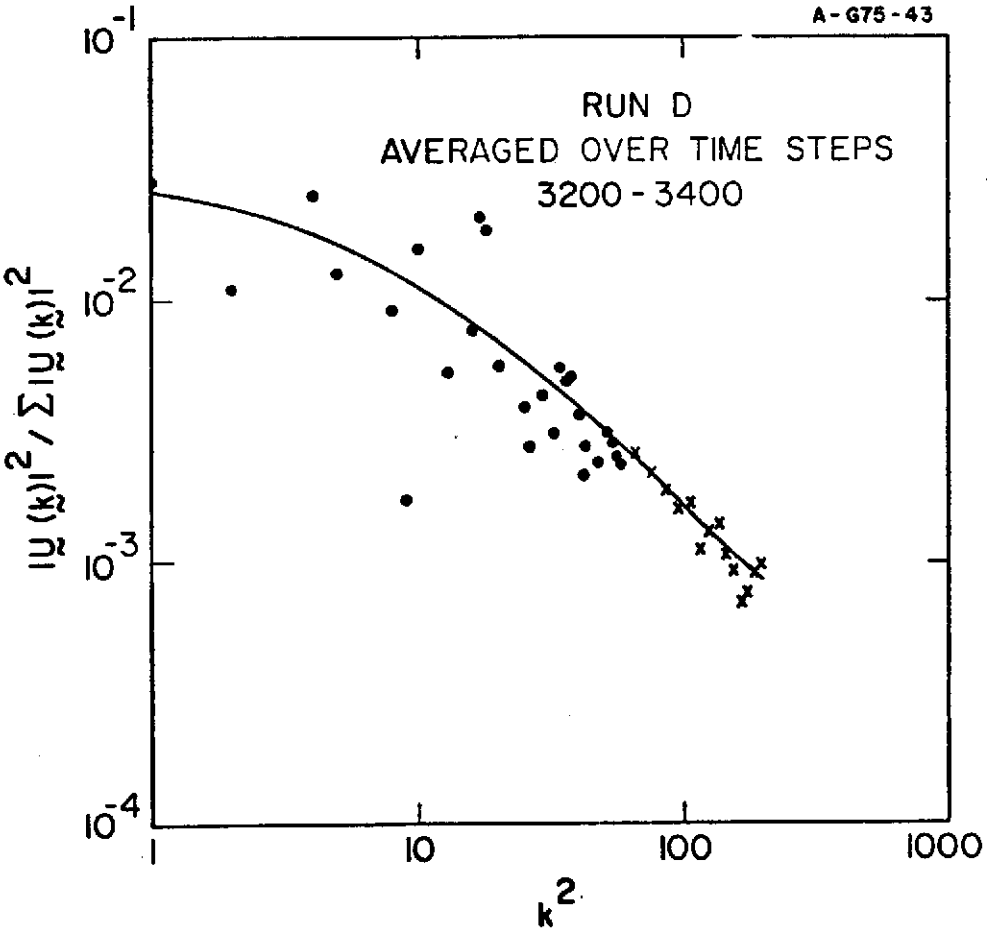
A-G75-43
RUN D
AVERAGED OVER TIME STEPS
3200 - 3400
10^{-1}
10^{-2}
10^{-3}
10^{-4}
$|\underset{\sim}{u}(k)|^2 / \Sigma|\underset{\sim}{u}(k)|^2$
1
10
100
1000
k^2

Figure 4c

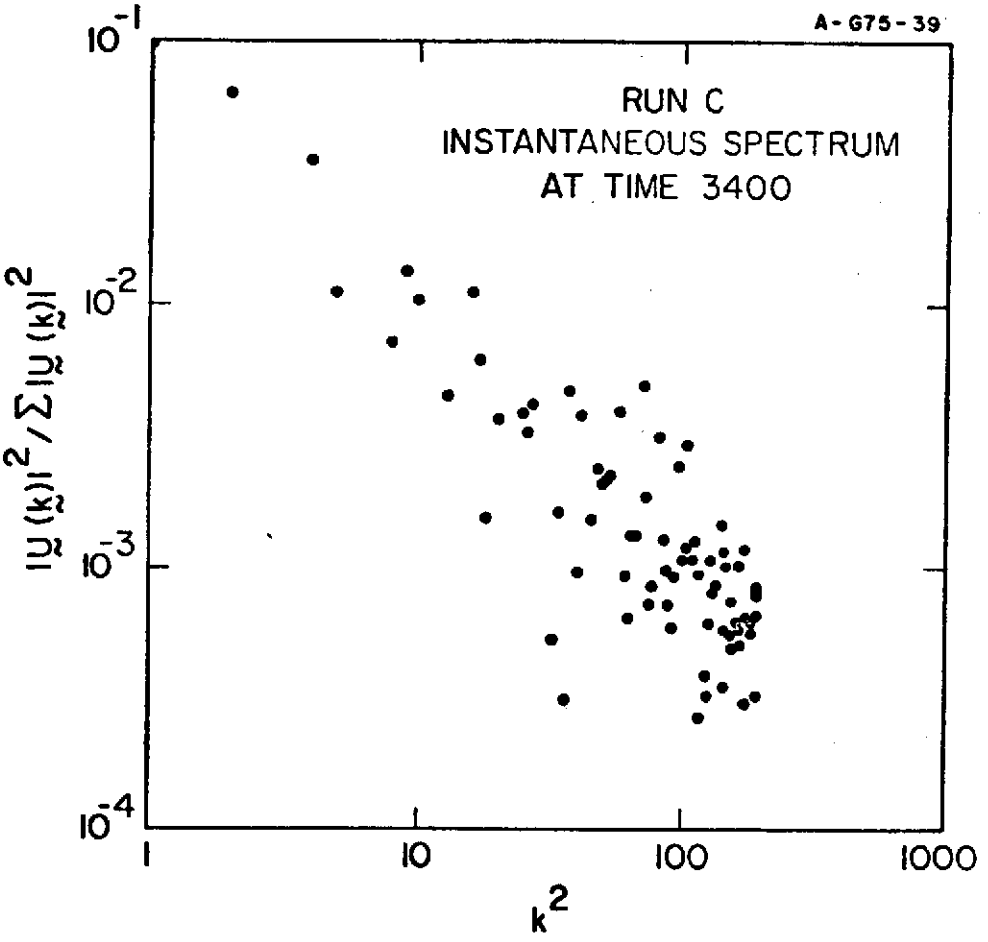
A-G75-39
RUN C
INSTANTANEOUS SPECTRUM
AT TIME 3400
10^{-1}
10^{-2}
10^{-3}
10^{-4}
$|\underset{\sim}{u}(k)|^2/\Sigma|\underset{\sim}{u}(k)|^2$
1
10
100
1000
k^2

Figure 5

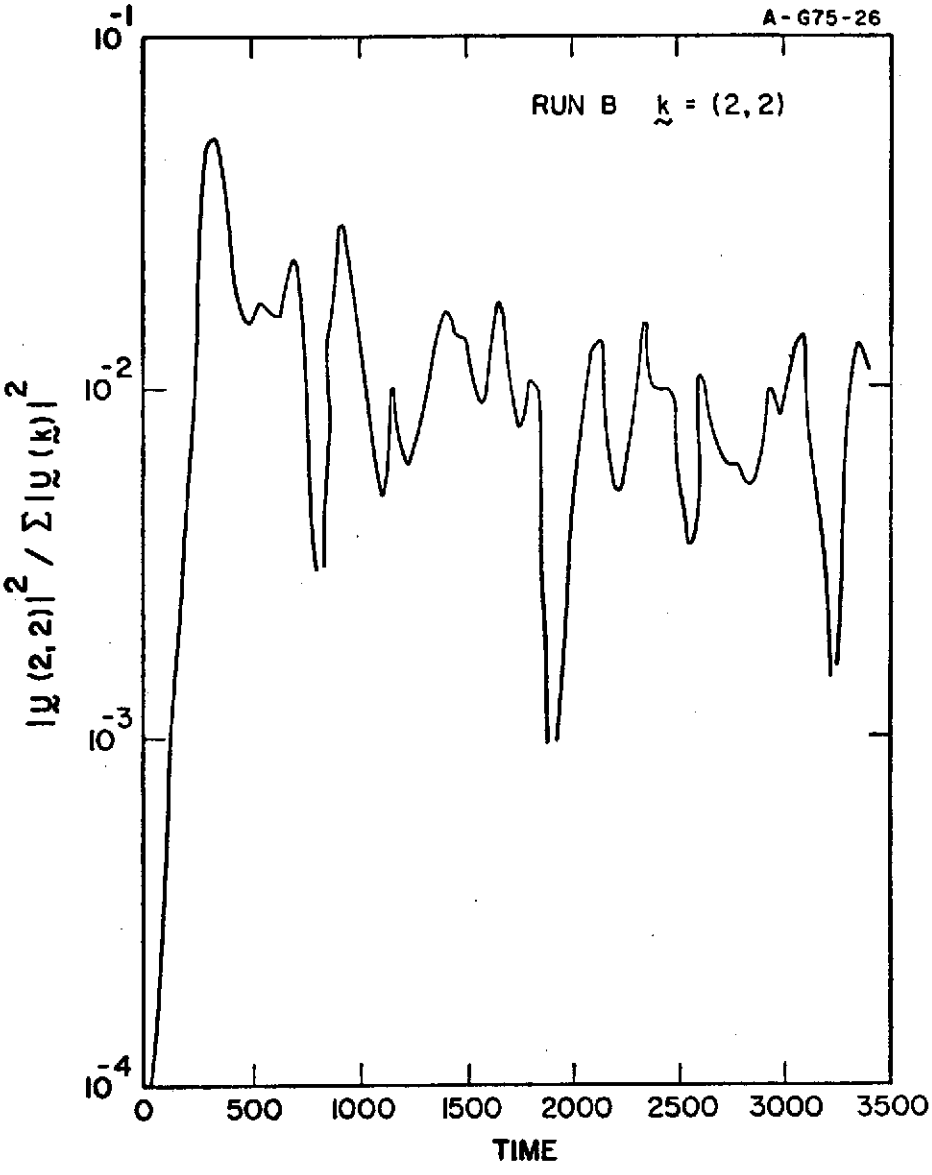
A-G75-26
RUN B k = (2,2)
10^{-1}
10^{-2}
10^{-3}
10^{-4}
$|\psi(2,2)|^2 / \Sigma|\psi(k)|^2$
0
500
1000
1500
2000
2500
3000
3500
TIME

Figure 6

Figure 7a

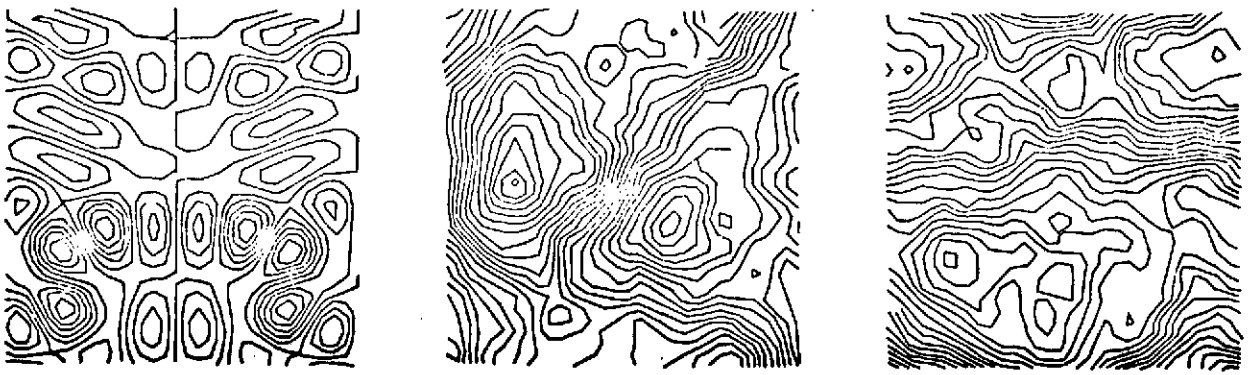

Figure 7b

B-G75-8

Figure 7c

Figure 7d

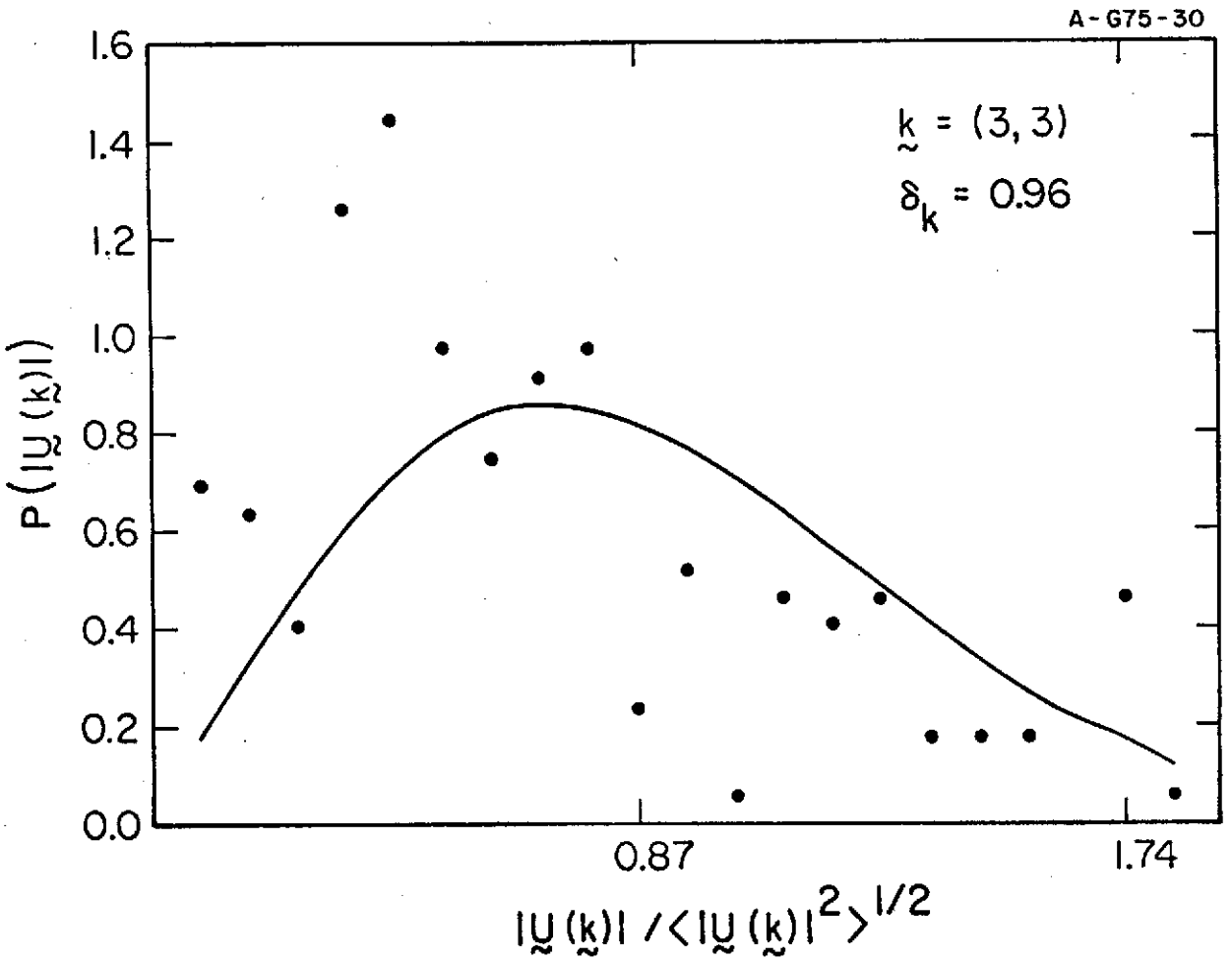

Figure 8a

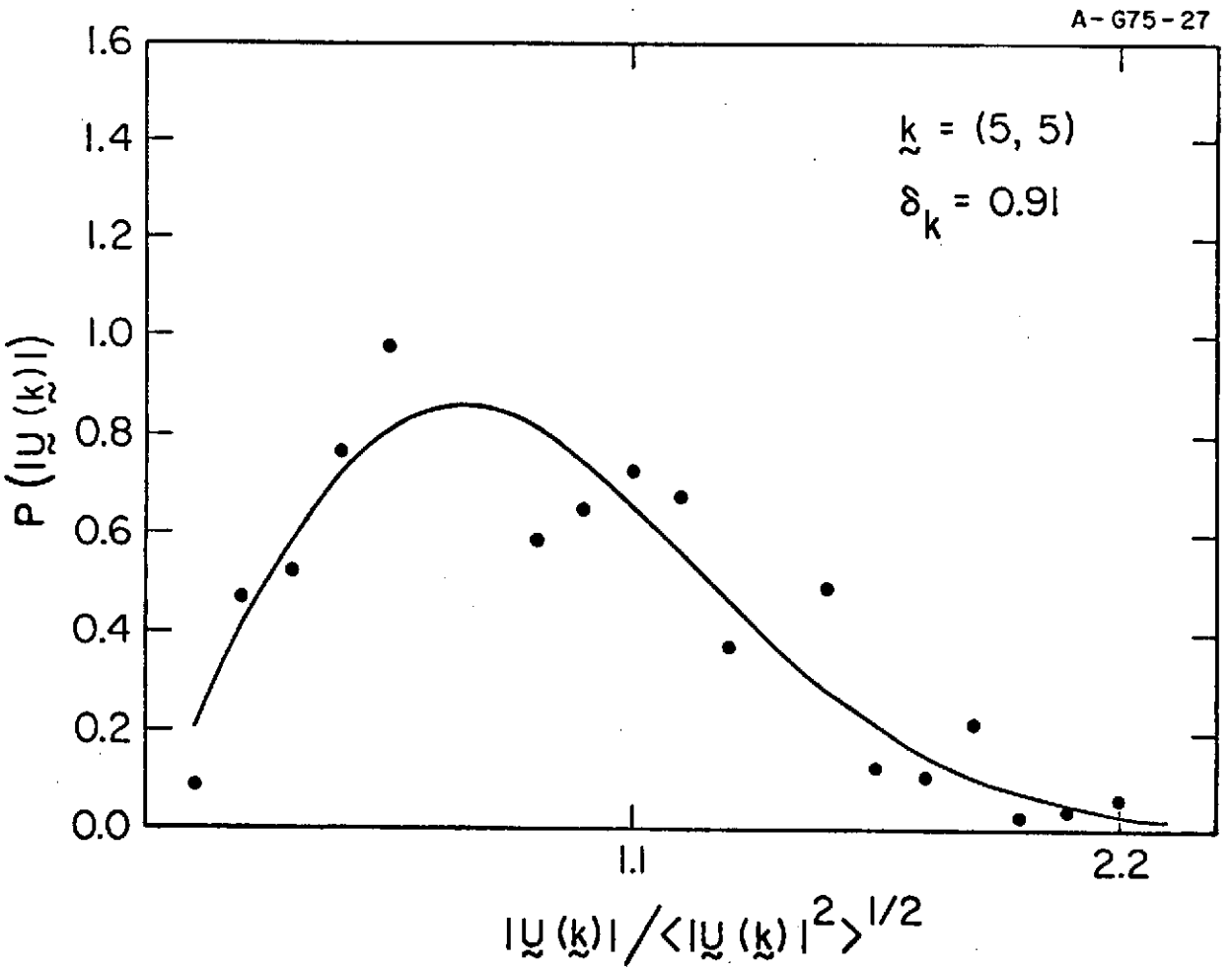

Figure 8b

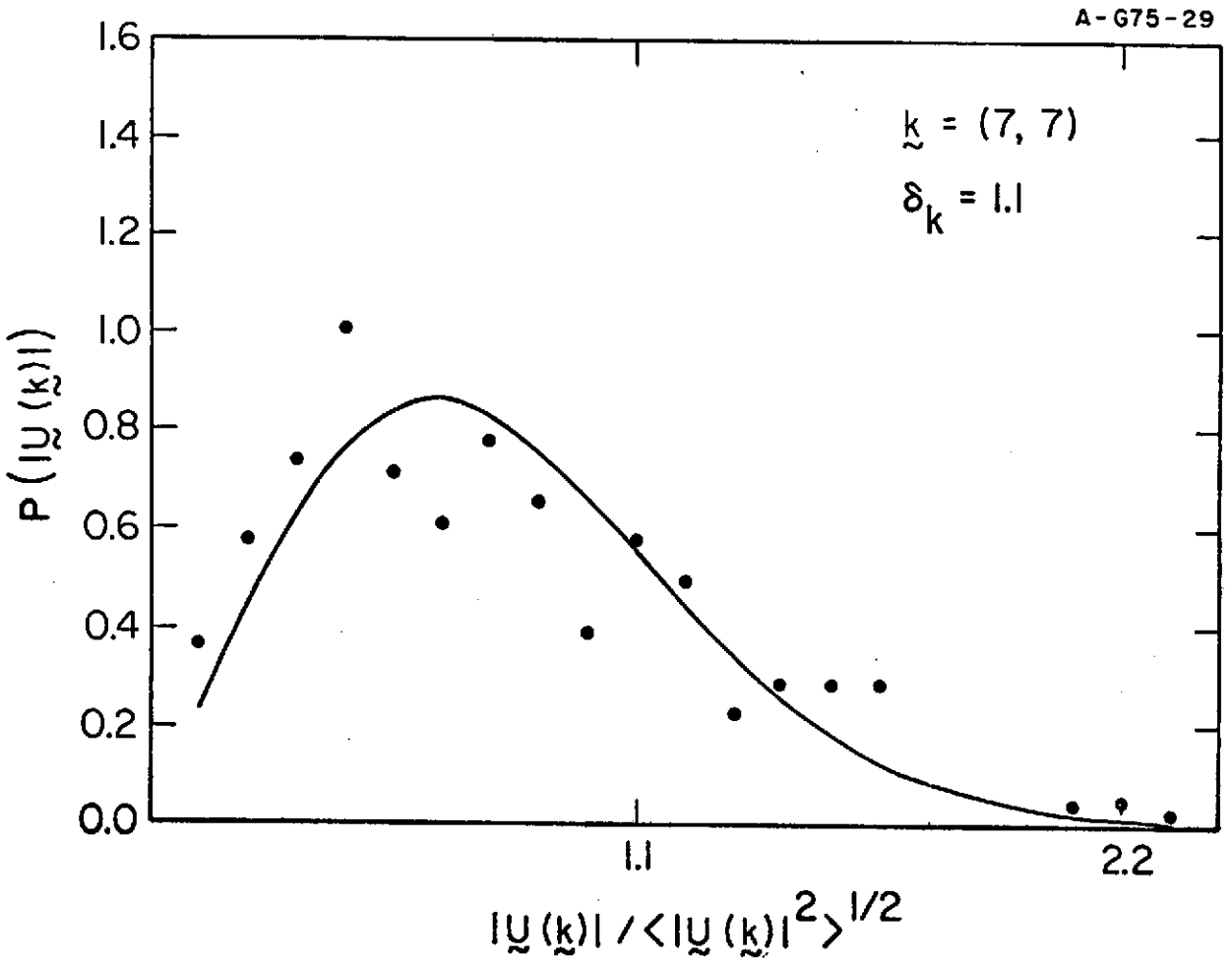

Figure 8c

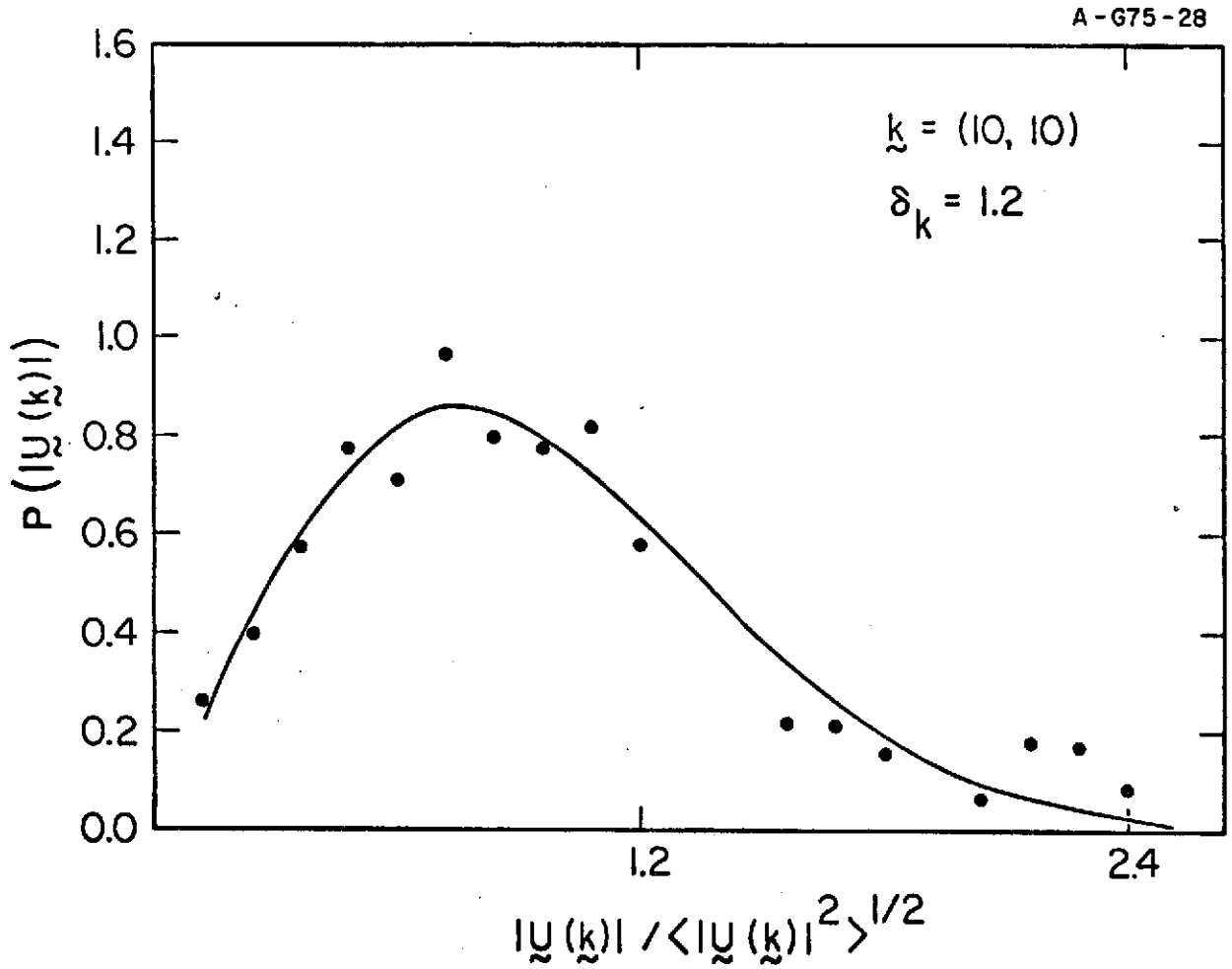

Figure 8d

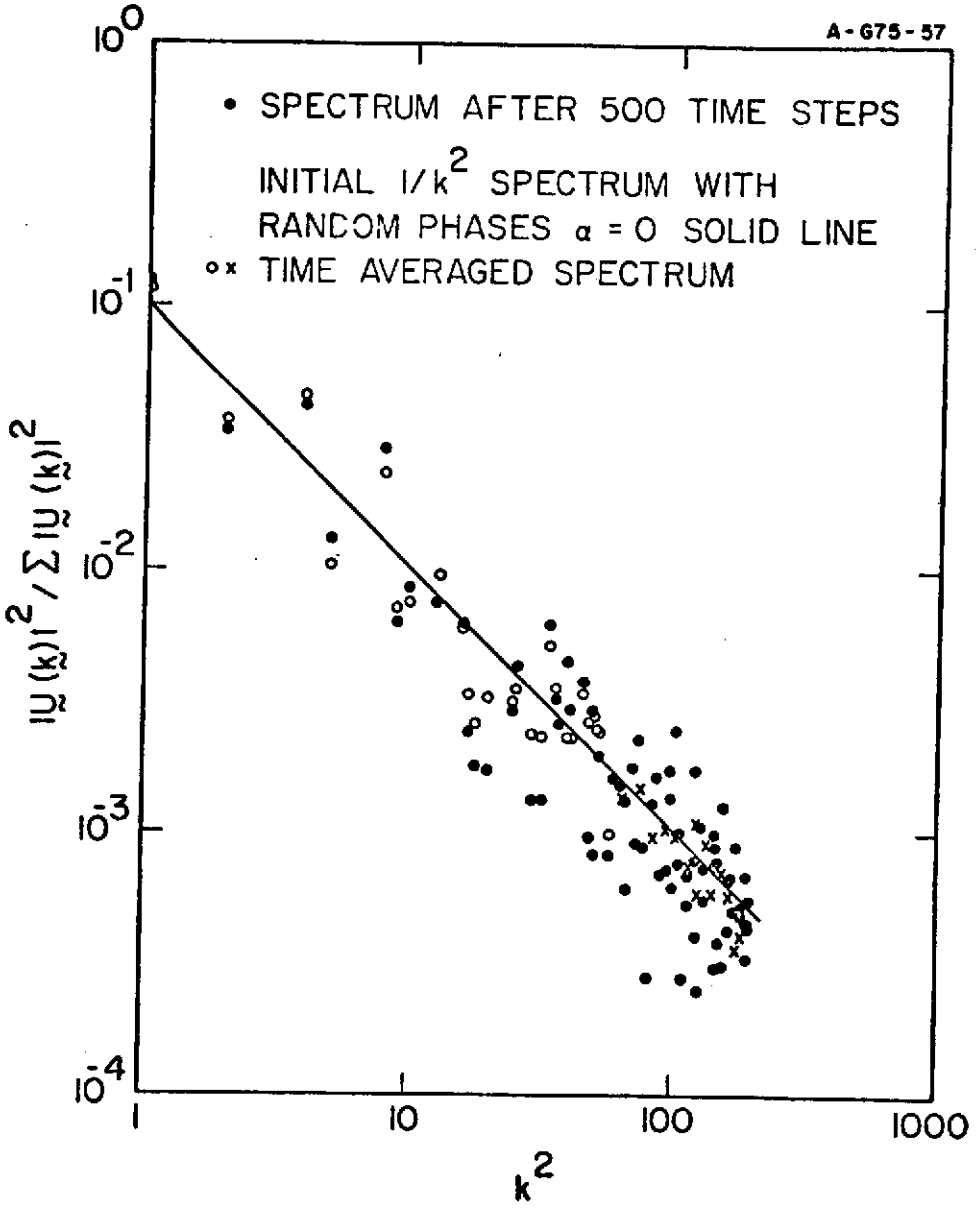
A-G75-57
• SPECTRUM AFTER 500 TIME STEPS
INITIAL $1/k^2$ SPECTRUM WITH
RANDOM PHASES $\alpha = 0$ SOLID LINE
o× TIME AVERAGED SPECTRUM
10^0
10^{-1}
10^{-2}
10^{-3}
10^{-4}
$|\underset{\sim}{u}(k)|^2 / \Sigma |\underset{\sim}{u}(k)|^2$
1
10
100
1000
k^2

Figure 9

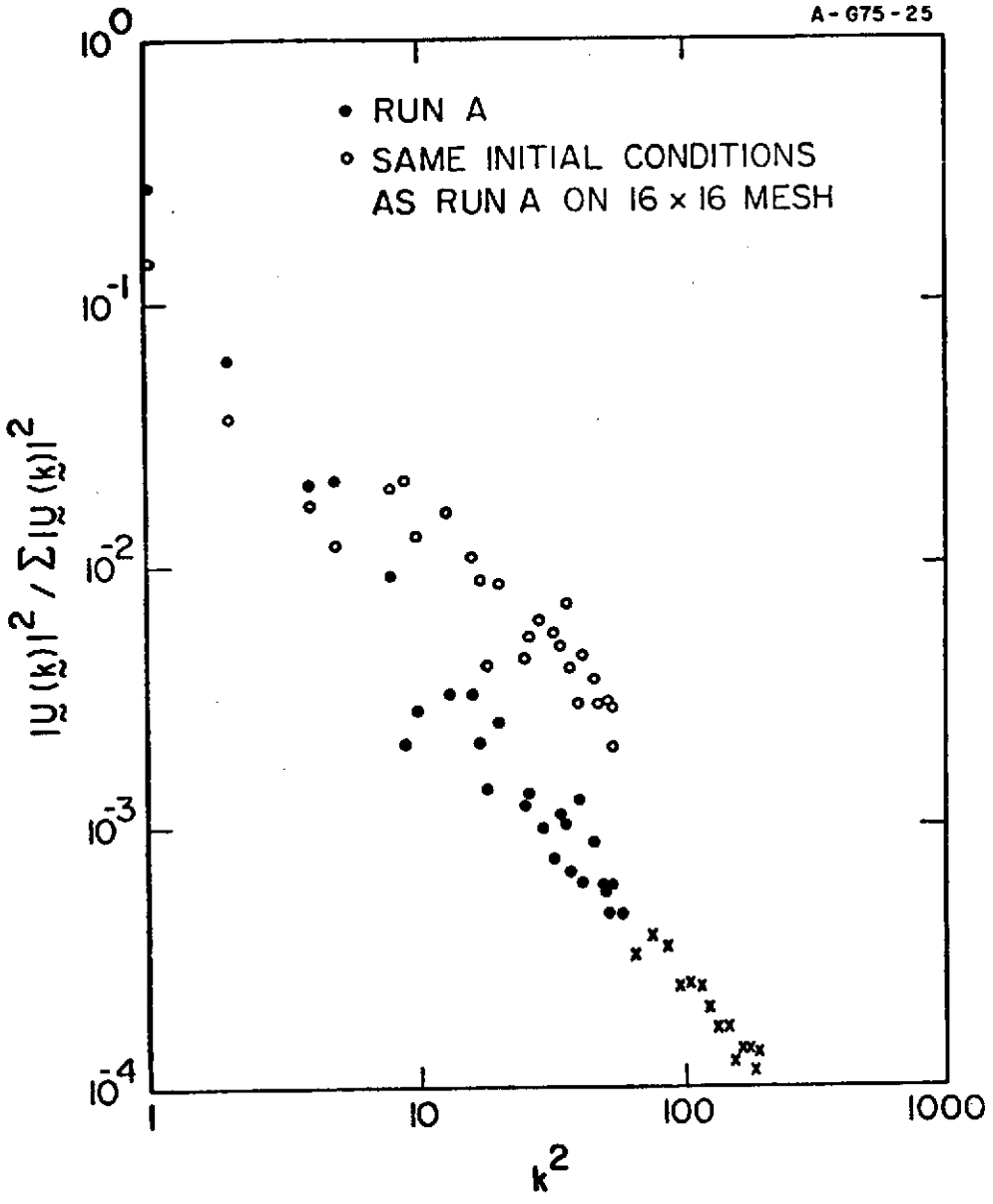
A-G75-25
• RUN A
○ SAME INITIAL CONDITIONS
AS RUN A ON 16 x 16 MESH
10^0
10^{-1}
10^{-2}
10^{-3}
10^{-4}
$|\underset{\sim}{u}(k)|^2 / \Sigma|\underset{\sim}{u}(k)|^2$
1
10
100
1000
k^2

Figure 10